

Department of Construction Sciences
Solid Mechanics

ISRN LUTFD2/TFHF-17/5221-SE(1-46)

Thermoplasticity in topology optimization based on finite strain

Master's Dissertation by
Anders Engström

Supervisors:
Supervisor, Professor Mathias Wallin

Examiner:
Examiner, Associate Professor Ralf Denzer

Copyright © 2017 by the Division of Solid Mechanics
and Anders Engström

Printed by Media-Tryck AB, Lund, Sweden

For information, address:

Division of Solid Mechanics, Lund University, Box 118, SE-221 00 Lund, Sweden

Webpage: www.solid.lth.se

Acknowledgements

This master thesis is submitted for Master degree in engineering in physics and was conducted between January 2017 and June 2017 at Division of Solid Mechanics, Faculty of engineering, Lund Univeristy. There are a few people I would like to thank. My supervisor Mathias Wallin for his time, interest in my work and his valuable suggestions on the work progress. Niklas Ivarsson for his patience and guidance during frustrating times. The lunch crew for the bantering. Friends and family for their non-ceasing support and love.

Lund, June 2017

Anders Engström

Abstract

A thermoplastic finite strain model is used to model heat generation due to plastic work. Isotropic hardening is used, where the mechanical dissipation acts as heat source in the heat equation. The multiplicative split of the deformation gradient makes it possible to separate plastic and elastic effects. The model is solved by using the Newmark time integration scheme with the finite element method using total Lagrangian formulation. The model is also aimed for implementation with gradient based topology optimization for finite strains with the objective to maximize the the plastic dissipation. The method of moving asymptotes (MMA) is used in the optimization to make the problem convex. The sensitivities required to form the gradient is calculated using the adjoint method where the sensitivities are derived for the thermoplastic case. Helmholtz's partial differential equation is used for regularization and a Heaviside filter is used to make the topology more precise.

Table of contents

List of figures	vii
List of tables	ix
Nomenclature	ix
1 Introduction	1
2 Thermoplasticity	3
2.1 Kinematics and multiplicative split	3
2.2 Free energy and local dissipation	4
2.3 Evolution equations and maximum dissipation	5
2.4 Temperature evolution - The heat equation	6
2.5 Application: von Mises J2-theory	7
2.6 Equilibrium equation	10
2.7 Virtual work	10
3 Numerical solution strategy	13
3.1 Finite element formulation	13
3.2 Non-linear solution procedure	14
3.3 Integration of Constitutive equations and the radial return method	16
4 Optimization	19
4.1 Material interpolation and regularization	20
4.2 Sensitivity analysis	21
4.2.1 Numerical differentiation	21
4.2.2 Adjoint method	21
4.3 Sensitivities of large strain thermoplasticity	27
4.3.1 Derivatives of outer residual	28

4.3.2	Derivatives of the local residual	30
4.3.3	Implicit derivatives of the objective function	33
4.3.4	The explicit term	34
4.4	Remarks about sensitivities	36
5	Results	37
6	Discussion	43
	References	45
	Appendix A Local solution	47
A.1	47
	Appendix B Derivation of the algorithmic stiffness tensor	49
	Appendix C Matrices in FE-formulation	51

List of figures

5.1	Double clamped beam used to illustrate the model.	37
5.2	Deformed topology for thermomechanical model with 0.8mm prescribed displacement in middle of structure	38
5.3	Generated temperature in the structure using the thermomechanical model with 0.8mm prescribed displacement	39
5.4	Generated plastic work in the structure using the thermomechanical model with 0.8mm prescribed displacement	40
5.5	Generated plastic work in the structure using the thermomechanical model with 0.8mm prescribed displacement	40
5.6	Deformed topology for thermomechanical model with 2.5mm prescribed disp.	41
5.7	Deformed topology, isothermal model with 2.5mm prescribed disp.	41
5.8	Generated temperature in the structure using the thermomechanical model with 2.5mm prescribed displacement	41
5.9	Generated plastic work in the structure using the thermomechanical model with 2.5mm prescribed displacement	42
5.10	Total generated plastic work in the structure using the thermomechanical model with 2.5mm prescribed displacement	42

List of tables

5.1	Material properties for steel	37
5.2	Comparison of the thermomechanical model using the sensitivities in [19] versus the numerically differentiated sensitivities for some prescribed displacement	38

Chapter 1

Introduction

Topology optimization is today used in the industry as a tool to develop designs early in the design process for structural problems. The most common objective is to maximize the stiffness of a structure. The vast majority of the commercial software for optimization is today restricted to optimizing of structures subjected to small deformations. In fact, most of the research has been focus on this area and only a very limited number of works, such as [19], have studied optimization for large deformations. General conditions such as finite strains is for instance of interest as large deformation arises in e.g. protective applications where the objective can be to maximize the mechanical dissipation of the structure. An example of this is in the automotive industry where deformation zones are used for absorbing energy in order to protect the passengers.

During large plastic deformations, the mechanical dissipation is converted into heat which then effect the material properties. In topology optimization, this coupling effect the final design and it is of interest to investigate this dependency. The aim of this master thesis is therefore to derive a theoretical framework for implementing thermoplasticity for use with finite strain topology optimization. The aim is also to evaluate for what conditions the isothermal assumption in the optimization performed by [19] is valid and to investigate in which part of a structure the accumulated temperature leads to changes in material properties, e.g thermal softening.

An associative, isotropic finite strain thermoplastic model is implemented in a finite element scheme as presented in [14]. Based on the work of [18] the heat generation is assumed to be a constant fraction of the plastic work. Moreover, it is assumed that the structure deforms rapidly, and therefore the conduction can be neglected which enables the temperature to be treated as an internal variable. The total Lagrangian formulation was used for the mechanical balance laws and solved for by using the

Newmark time integration scheme. The constitutive equations were integrated using Euler backward scheme.

In order to use convex programming, a sequence of separable convex approximations is formed using the method of moving asymptotes (MMA) cf. [16]. As the problem is path-dependent, so are the sensitivities and this needs special attention which is dealt with. The sensitivities used for forming the gradient are derived using the adjoint procedure as presented in [11]. Furthermore, a filter is introduced for regularization by solving the Helmholtz's PDE as presented in [10] and a Heaviside thresholding was used to solve the problem with intermediate designs in the transition from void material to full material see e.g. [2].

Chapter 2

Thermoplasticity

2.1 Kinematics and multiplicative split

Let the particles in the reference configuration $\Omega_0 \subset \mathbb{R}^3$ be labeled by a position vector \mathbf{X} and let φ denote the mapping from the reference configuration to the deformed configuration \mathbf{x} like $\varphi : \Omega_0 \rightarrow \Omega \subset \mathbb{R}^3$. The deformation gradient $\mathbf{F} = \partial_{\mathbf{X}}\varphi$ maps the line segment $d\mathbf{R}$ in the reference configuration to the line segment $d\mathbf{r}$ in the deformed configuration like $d\mathbf{r} = \mathbf{F}d\mathbf{R}$. The Jacobian is defined as $J = \rho_0/\rho = \det(\mathbf{F})$ where ρ_0 and ρ is the density in the reference configuration and the deformed configuration respectively. In order to measure the deformation and strain, introduce the Cauchy deformation tensor, \mathbf{C} , and the Green-Lagrange strain tensor, \mathbf{E} as

$$\mathbf{C} = \mathbf{F}^T \mathbf{F}, \quad \mathbf{E} = \frac{1}{2}(\mathbf{C} - \mathbf{1}). \quad (2.1)$$

For large strains the additive split of the strain tensor can not be used. To separate the elastic deformation from the plastic, use is therefore made of the multiplicative decomposition of the deformation gradient $\mathbf{F} = \mathbf{F}^e \mathbf{F}^p$ (cf. in eg. [8]) where \mathbf{F}^e is the elastic part and \mathbf{F}^p is the plastic part. During plastic deformation, \mathbf{F}^e describes recoverable deformation such as reversible distortion of the crystal whereas \mathbf{F}^p describes non-recoverable deformation such as dislocation movements. The deformation gradient is also split in a volumetric part and an isochoric part as $\bar{\mathbf{F}} = J^{2/3} \mathbf{F}$. The following two strain measures are also used in the following report

$$\mathbf{G}^p = [\mathbf{F}^{pT} \mathbf{F}^p]^{-1} \quad \text{and} \quad \mathbf{b}^e := \mathbf{F}^e \mathbf{F}^{eT} \quad (2.2)$$

where \mathbf{b}^e is the push-forward of \mathbf{G}^p to the current configuration as

$$\mathbf{b}^e = \mathbf{F}\mathbf{G}^p\mathbf{F}^T. \quad (2.3)$$

Time differentiation of 2.2 gives the following expression

$$\dot{\mathbf{b}}^e = \mathbf{l}\mathbf{b}^e + \mathbf{b}^e\mathbf{l}^T + \mathcal{L}_v\mathbf{b}^e \quad (2.4)$$

where the Lie derivative is defined as $\mathcal{L}_v\mathbf{b}^e := \mathbf{F}\dot{\mathbf{G}}^p\mathbf{F}^T$ and the spatial velocity gradient is defined as $\mathbf{l} := \dot{\mathbf{F}}\mathbf{F}^{-1}$.

2.2 Free energy and local dissipation

To identify the state of the body, use is made of as set of state variables $\mathbf{w} = [\mathbf{b}^e, \alpha, \theta]$. The state variables include the elastic left Cauchy-Green tensor $\mathbf{b}^e = \mathbf{F}^e(\mathbf{F}^e)^T$ as well as the internal variable α used to model the isotropic hardening and, as will be dealt with later, the temperature θ . To describe these, together with the entropy, the internal energy function is introduced as

$$e = \hat{e}(\mathbf{b}^e, \alpha, s^e), \quad \text{where} \quad s^e := s - s^p \quad (2.5)$$

The Helmholtz's free energy function is then obtained from the internal energy 2.5 by a Legendre transformation as

$$\Psi(\mathbf{w}, \theta) = e(\mathbf{w}, s^e) - s^e\theta. \quad (2.6)$$

The Clausius-Plank form of the second law of thermodynamics is

$$\gamma := \theta\gamma_{loc} := \theta\dot{s} + \boldsymbol{\tau} : \mathbf{D} - \dot{e} \geq 0, \quad (2.7)$$

where γ_{loc} is the local entropy production, \mathbf{D} is the rate of deformation tensor as $\mathbf{D} = 1/2(\mathbf{l} + \mathbf{l}^T)$ and $\boldsymbol{\tau}$ is the Kirchhoff stress. This is valid assuming positive dissipation due to heat conduction, i.e. $\theta\gamma_{cond} := -\mathbf{q}\nabla\theta/\theta \geq 0$. Differentiation of the free energy function 2.6 and insertion of the time differentiation of the left Cauchy

-Green tensor \mathbf{b}^e in 2.4 as

$$\dot{\Psi} = \partial_{\mathbf{b}^e} \Psi \dot{\mathbf{b}}^e + \partial_\alpha \Psi \dot{\alpha} + \partial_\theta \Psi \dot{\theta} \quad (2.8)$$

$$= [\partial_{\mathbf{b}^e} \Psi \mathbf{b}^e] : [2\mathbf{I} + (\mathcal{L}\mathbf{b}^e)\mathbf{b}^{e-1}] + \partial_\theta \Psi \dot{\theta} + \partial_\alpha \Psi \dot{\alpha}. \quad (2.9)$$

Differentiate the free energy function from 2.6

$$\dot{\Psi} = \dot{e} - \dot{s}\theta \quad (2.10)$$

and insert this into the dissipation inequality 2.7 to form

$$\begin{aligned} \gamma = & [-(s - s^p) - \partial_\theta \Psi] \dot{\theta} + [\boldsymbol{\tau} - 2\partial_{\mathbf{b}^e} \Psi] : \mathbf{D} \\ & + [2\partial_{\mathbf{b}^e} \Psi \mathbf{b}^e] : \left[-\frac{1}{2} (\mathcal{L}_v \mathbf{b}^e) \mathbf{b}^{e-1} \right] + [\partial_\alpha \Psi] \dot{\alpha} + \theta \dot{s}^p \geq 0 \end{aligned} \quad (2.11)$$

If 2.11 is to always hold, the first and second term must be zero, which gives the constitutive equation

$$\boldsymbol{\tau} = 2\partial_{\mathbf{b}^e} \Psi \mathbf{b}^e \quad s = s^p - \partial_\theta \Psi \mathbf{b}^e \quad (2.12)$$

and the dissipation expression in 2.11 is reduced to

$$\gamma = \underbrace{\boldsymbol{\tau} : \left[-\frac{1}{2} (\mathcal{L}_v \mathbf{b}^e) \mathbf{b}^{e-1} \right] - \partial_\alpha \Psi \dot{\alpha}}_{\gamma_{mech}^{def}} + \underbrace{\theta \dot{s}^p}_{\gamma_{therm}^{def}} \quad (2.13)$$

The first term γ_{mech}^{def} is the standard contribution to the dissipation in the purely mechanical theory, while the second term γ_{therm}^{def} is associated with the entropy production.

2.3 Evolution equations and maximum dissipation

In order to define the evolution laws for the internal variables use is made of the principle of maximum dissipation (see eg. [5] p.60). The classic principle of maximum dissipation results in associative plasticity. Consider the fixed state $(\boldsymbol{\tau}, \beta, \theta)$ in a plastically deformed structure where $\beta = \partial_\alpha \Psi$. Assume that the intermediate configuration with $\mathbf{b}^e = \mathbf{F}\mathbf{G}^p\mathbf{F}^T$ and \mathbf{F}^p are known together with the rates $\mathcal{L}_v \mathbf{b}^e, \dot{\alpha}, \dot{s}^p$. Maximization of

the dissipation gives the evolution equations for \mathbf{b}^e and α as

$$-\frac{1}{2}\mathcal{L}_v\mathbf{b}^e = \lambda[\partial_\tau f]\mathbf{b}^e, \quad \dot{\alpha} = \lambda\partial_\beta f \quad (2.14)$$

where f is the yield function. For more information about the postulate see eg. [14] or [7].

2.4 Temperature evolution - The heat equation

Following for example [3], [14] the heat equation governing the temperature influence of the deformation can be derived using the second and the first law of thermodynamics. The first law of thermodynamics is a conservation law of energy which yields a coupling between the mechanical deformation field and the temperature field $\theta(\mathbf{x}, t)$. The local form of the first law of thermodynamics in the current configuration is expressed as

$$\dot{e} = \boldsymbol{\tau} : \mathbf{D} + r - J\text{div}(\mathbf{q}/J) \quad (2.15)$$

where r is a heat source and \mathbf{q} is the heat flux vector. Substitution of the second law of thermodynamics 2.7 into the first law of thermodynamics results in

$$\theta(\dot{s} - \dot{s}^p) - \gamma_{mech}^{def} = r - J\text{div}(\mathbf{q}/J) \quad (2.16)$$

where use is made of $\dot{\psi} = \boldsymbol{\tau} : \mathbf{D} - \gamma_{mech}^{def} - \dot{\theta}s^e$ which follows from 2.11. Differentiation of the second constitutive relation 2.12 results in the evolution of the total entropy

$$\theta\dot{s} = \theta\dot{s}^p + c\dot{\theta} + \mathcal{H} \quad (2.17)$$

where $c = -\theta\partial_{\theta\theta}^2\Psi$ and $\mathcal{H} = -\theta[\partial_{\theta\mathbf{b}^e}\Psi\dot{\mathbf{b}}^e + \partial_{\theta\alpha}\Psi\dot{\alpha}]$ were introduced. Substituting 2.17 into 2.16 results in the temperature evolution equation as

$$c\dot{\theta} = [\gamma_{mech}^{def} - \mathcal{H}] + [-J\text{div}[\mathbf{q}/J] + r]. \quad (2.18)$$

Insertion of Fourier' law $\mathbf{q} = -k\nabla\theta$ in 2.18 results in the heat equation.

Considering the problem at hand, the external heat source is not present i.e. $r = 0$. The structure is also assumed to deform rapidly such as the spatial heat flow is small and therefore can be neglected i.e. $\mathbf{q} = \mathbf{0}$. When the heat flow is neglected it enables the temperature to be treated as a state variable and not a field variable. Based on

these two assumptions the heat equation can be approximated as

$$\rho_0 c \dot{\theta} = \eta \gamma_{mech} \quad (2.19)$$

where the factor η is introduced as compensation for the neglected terms and $\gamma_{mech} = \boldsymbol{\tau} : \mathbf{D} - \rho_0 \partial_\alpha \Psi \dot{\alpha}$ is the mechanical dissipation expressed in the reference configuration. This factor is often assumed to be constant between 0.85 – 0.95, a practice that dates back to the early work of [18]. Many later works have shown this approximation is not in perfect agreement with experimental findings see eg. [12] where it is concluded that η depends on the accumulated plastic strain. The variation of η is most significant for small and moderate strains and since [18] did their experiments for large strain, this variation was not perceived. The simplifying assumption is still used in most commercial FE-codes and will also be employed in this work. The total plastic work for the structure is found by summarizing all the contributions in the structure spatially, as well as in time like

$$W^p = \int_0^T \int_{\Omega_0} \gamma_{mech} dt dV \quad (2.20)$$

where T is the time when the structure is fully loaded.

2.5 Application: von Mises J2-theory

The theory presented above can be used in a thermomechanical model of J_2 -flow theory (von Mises-flow theory) for finite strains as done in [14]. The specific form of the free energy function in 2.6 is assumed to be

$$\Psi = \underbrace{T(\theta) + M(J, \theta)}_{thermal} + \underbrace{U(J) + W(\bar{\mathbf{b}}^e)}_{hyperelastic} + \underbrace{K(\alpha)}_{hardening} . \quad (2.21)$$

The thermoelastic free energy $\Psi^e = T + M + U + W$ is decoupled from plastic contribution $\Psi^p = K$ which includes the hardening variables. This is common practice for J_2 -flow metal-plasticity and can be explained physically by the lattice structure associated with thermoelastic response being close to unaffected by the plastic response. The hyperelastic model used is isotropic as

$$U(J) = \kappa \left[\frac{1}{2} (J^2 - 1) - \ln(J) \right], \quad W(\mathbf{b}^e) = \frac{1}{2} \mu [tr[\bar{\mathbf{b}}^e] - 3] \quad (2.22)$$

where κ is the shear modulus and μ the bulk modulus. These two quantities represent the volumetric/deviatoric part respectively of the elasticity, a common split of the elastic

response in metal plasticity. Regarding the first two terms an explicit expression for these can be achieved if the specific heat capacity c is assumed constant. Differentiating the free energy function with respect to the temperature, following [14] it follows that

$$M(J, \theta) = (\theta - \theta_0)G(J) \quad (2.23)$$

where $G(J) = -3\beta U'(J)$ describes the models the thermal expansion and θ_0 represents the reference temperature.

With this specific choice of energy function 2.22, the stress can now be calculated from 2.12 as

$$\boldsymbol{\tau} = 2\partial_{\mathbf{b}^e}\Psi = pJ\mathbf{1} + \text{dev}[\boldsymbol{\tau}] \quad (2.24)$$

where the stress has been split up into a volumetric part and a deviatoric part as

$$p := U'(J) + \partial_J M(\theta, J) \quad (2.25)$$

$$\text{dev}[\boldsymbol{\tau}] = 2\text{dev}[\bar{\mathbf{b}}^e \partial_{\bar{\mathbf{b}}^e} W(\bar{\mathbf{b}}^e)] = \mu \text{dev}[\bar{\mathbf{b}}^e] \quad (2.26)$$

To describe the transition from elastic to elasto-plastic response, the von-Mises yield function is used

$$f(\boldsymbol{\tau}, \alpha, \theta) = \|\text{dev}[\boldsymbol{\tau}]\| - \sqrt{\frac{2}{3}} \left(\hat{K}'(\alpha, \theta) + \hat{\sigma}_{y_0}(\theta) \right) \leq 0 \quad (2.27)$$

where the initial yield stress $\hat{\sigma}_{y_0}$ and the hardening function $\hat{K}'(\alpha, \theta)$, that describes the isotropic hardening mechanism, are

$$\hat{K}'(\alpha, \theta) = \hat{h}(\theta)\alpha^m + \hat{\sigma}_{y_\infty}(\theta)(1 - e^{-\delta\alpha}). \quad (2.28)$$

In the expression above $\hat{h}(\theta)$ is the hardening modulus, $\hat{\sigma}_{y_\infty}(\theta)$ is the saturation hardening, δ and m are hardening exponents. To introduce a temperature dependence in the parameters a linear relation is introduced that implies relative small change with temperature, i.e.

$$\hat{\sigma}_{y_0} = \sigma_{y_0}[1 - \omega_0(\theta - \theta_0)] \quad (2.29)$$

$$\hat{h} = h[1 - \omega_h(\theta - \theta_0)] \quad (2.30)$$

$$\hat{\sigma}_{y_\infty} = \sigma_{y_\infty}[1 - \omega_h(\theta - \theta_0)] \quad (2.31)$$

where ω_0 and ω_h are parameters that describe the temperature influence. This assumption is reasonable for most steels according to experimental findings from e.g. [20]. The hardening function with temperature dependent parameters is thus expressed as

$$\hat{K}'(\alpha, \theta) = h[1 - \omega_h(\theta - \theta_0)]\alpha^m + \sigma_{y\infty}[1 - \omega_h(\theta - \theta_0)](1 - e^{-\delta\alpha}). \quad (2.32)$$

Considering the first equation in 2.14. Calculating this with the von Mises yield criterion and decomposing $\bar{\mathbf{b}}^e$ into deviatoric and spherical parts, the first flowrule turns into

$$\mathcal{L}_v \mathbf{b}^e = -2\lambda J^{2/3} \left[\frac{1}{3} \text{tr}[\bar{\mathbf{b}}^e] \mathbf{n} + \frac{\|\text{dev}[\boldsymbol{\tau}]\|}{\mu} \mathbf{n}^2 \right] \quad (2.33)$$

where

$$\mathbf{n} := \text{dev}[\boldsymbol{\tau}] / \|\text{dev}[\boldsymbol{\tau}]\|. \quad (2.34)$$

The second term in the bracket of 2.33 can be neglected following [14] since $\|\text{dev}[\boldsymbol{\tau}]/\mu\|$ is of magnitude equal to the flow stress divided by the shear modulus ($\sim 10^3$). The result is shown in the first equation in 2.36. The second equation in the evolution equations in 2.14 with the chosen von-Mises yield function results in the second equation in 2.36.

By substituting the first evolution equation in 2.14 into the dissipation inequality in 2.13 using the Kuhn-Tucker condition $\lambda f = 0$ (see eg. [14]) the thermomechanical dissipation takes the form

$$\gamma_{mech} := -\boldsymbol{\tau} \mathbf{b}^{e-1} \cdot \frac{1}{2} \mathcal{L}_v \mathbf{b}^e + \partial_\alpha \Psi \dot{\alpha} = \sqrt{\frac{2}{3}} \hat{\sigma}(\theta) \lambda. \quad (2.35)$$

Inserting this into the heat equation 2.19 result in the last equation in 2.36.

$$\begin{aligned} \mathbf{F} \dot{\mathbf{G}}^P \mathbf{F}^T &= -2\Delta\lambda \frac{1}{3} \text{tr}(\bar{\mathbf{b}}^e) \mathbf{n} && \text{flow rule} \\ \dot{\alpha} &= \lambda \sqrt{\frac{2}{3}} && \text{evolution for } \alpha \\ f &= \|\text{dev}(\boldsymbol{\tau})\| - \sqrt{\frac{2}{3}} (\hat{K}'(\alpha, \theta) + \hat{y}(\theta)) && \text{yield function} \\ \dot{\theta} &= \frac{\eta}{\rho_0 c} \sqrt{\frac{2}{3}} \hat{\sigma}(\theta) \lambda && \text{Heat equation} \end{aligned} \quad (2.36)$$

2.6 Equilibrium equation

Balance of the linear momentum for a body Ω in the deformed configuration can be written as

$$\int_{\Omega} \mathbf{t} ds + \int_{\Omega} \rho \mathbf{b} dv = \int_{\Omega} \rho \ddot{\mathbf{u}} dv \quad (2.37)$$

where \mathbf{t} is the traction vector, \mathbf{b} is the body force and $\ddot{\mathbf{u}}$ is the acceleration. Applying Cauchy's theorem and the divergence theorem

$$\mathbf{t} = \boldsymbol{\sigma} \mathbf{n} \quad \int_{\Omega} \boldsymbol{\sigma} \mathbf{n} ds = \int_{\Omega} \operatorname{div} \boldsymbol{\sigma} dv \quad (2.38)$$

where $\boldsymbol{\sigma}$ is the Cauchy stress tensor results in

$$\int_{\Omega} (\boldsymbol{\sigma} + \rho \mathbf{b} - \rho \ddot{\mathbf{u}}) dv = 0. \quad (2.39)$$

This holds for arbitrary volume and thus arbitrary point, and the equation of motion is formed

$$\operatorname{div}(\boldsymbol{\sigma}) + \rho \mathbf{b} - \rho \ddot{\mathbf{u}} = 0. \quad (2.40)$$

2.7 Virtual work

The strong form in 2.40 isn't suitable for FE implementation, thus an effort is made to derive the weak form. Multiplication of the equation of motion with an virtual displacement $\delta \mathbf{u}$ and integrating this over the deformed configuration results in

$$\int_v \delta \mathbf{u}^T \operatorname{div}(\boldsymbol{\sigma}) dv + \int_v \delta \mathbf{u}^T \rho \mathbf{b} dv = \int_v \delta \mathbf{u}^T \rho \ddot{\mathbf{u}} dv. \quad (2.41)$$

Using Cauchy's theorem and inserting the divergence theorem together with Green-Gauss's theorem yields

$$\int_s \delta \mathbf{u}^T \mathbf{t} ds - \int_v \frac{1}{2} (\nabla \delta \mathbf{u} + (\nabla \delta \mathbf{u})^T) : \boldsymbol{\sigma} dv + \int_v \delta \mathbf{u}^T \rho \mathbf{b} dv = \int_v \delta \mathbf{u}^T \rho \ddot{\mathbf{u}} dv. \quad (2.42)$$

If the total Lagrangian description is to be used, the equation needs to be expressed in the reference configuration. Considering the terms, starting with the body force, the volume integral and the density can be rewritten as

$$\int_v \rho \delta \mathbf{u}^T \mathbf{b} dv = \int_{v_0} \rho_0 \delta \mathbf{u}^T \mathbf{b} dv_0. \quad (2.43)$$

The term including the traction force and the acceleration is transformed in a similar way. For the second term, Cauchy's theorem and Nanson's formula can be used to rewrite it to the desired form

$$\int_s \delta \mathbf{u}^T \mathbf{t} ds = \int_s \delta \mathbf{u}^T \boldsymbol{\sigma} \mathbf{n} ds = \int_{s_0} \delta \mathbf{u}^T J \boldsymbol{\sigma} \mathbf{F}^{-T} \mathbf{n}_0 ds_0 = \int_{s_0} \delta \mathbf{u}^T \mathbf{P} \mathbf{n}_0 ds_0 = \int_{s_0} \delta \mathbf{u}^T \mathbf{t}_0 ds_0 \quad (2.44)$$

where \mathbf{F} is the deformation gradient and \mathbf{P} is the first Piola Kirchhoff stress. If $\delta \mathbf{E}_\square$ is introduced as

$$\frac{1}{2}(\nabla \delta \mathbf{u} + (\nabla \delta \mathbf{u})^T) = \mathbf{F}^{-T} \delta \mathbf{E}_\square \mathbf{F}^{-1} \quad (2.45)$$

the second term can be expressed as

$$\int_v \frac{1}{2}(\nabla \delta \mathbf{u} + (\nabla \delta \mathbf{u})^T) : \boldsymbol{\sigma} dv_0 = \int_{v_0} \delta \mathbf{E}_\square : \mathbf{S}_\square dv \quad (2.46)$$

where the second Piola Kirchhoff stress can be written as

$$\mathbf{S}_\square = \mathbf{F}^T \boldsymbol{\tau} \mathbf{F} \quad (2.47)$$

This results in the virtual work in the reference configuration, suitable for FE-formulation

$$\mathcal{V} = \int_{V_0} \rho_0 \delta \mathbf{u}^T \ddot{\mathbf{u}} dV_0 + \int_{V_0} \delta \mathbf{E}_\square : \mathbf{S}_\square dV_0 - \int_{S_0} \delta \mathbf{u}^T \mathbf{t}^0 dS_0 - \int_{V_0} \rho_0 \delta \mathbf{u}^T \mathbf{b} dV_0 = 0. \quad (2.48)$$

Chapter 3

Numerical solution strategy

3.1 Finite element formulation

The virtual work in 2.48 is discretized spatially by the finite element method. Introducing shape functions \mathbf{N} as $\mathbf{u} = \mathbf{N}\hat{\mathbf{u}}$, $\mathbf{v} = \mathbf{N}\hat{\mathbf{v}}$, and $\mathbf{a} = \mathbf{N}\hat{\mathbf{a}}$ together with the Galerkin method results in the FE-formulation

$$\mathbf{R}(\hat{\mathbf{u}}, \hat{\mathbf{a}}) = \mathbf{M}\hat{\mathbf{a}} + \mathbf{F}_{int} - \mathbf{F}_{ext} \quad (3.1)$$

where $\delta\mathbf{E} = \mathbf{B}_0\delta\hat{\mathbf{u}}$

$$\mathbf{M} = \int_{\Omega_0} \rho \mathbf{N}^T \mathbf{N} dV_0, \quad (3.2)$$

$$\mathbf{F}_{int} = \int_{\Omega_0} \mathbf{B}_0^T \mathbf{S} dV, \quad (3.3)$$

$$\mathbf{F}_{ext} = \int_{\partial\Omega} \mathbf{N}^T \mathbf{t}^0 dS \quad (3.4)$$

and \mathbf{B}_0 is associated with the shape function see the Appendix C for more details where the form functions have been denoted for a 4-node element for convenience, or e.g. [13]. Approximations for $\hat{\mathbf{a}}$ is needed and in this work the Newmark time integration scheme is used. Using generalized trapezoidal rules the Newmark method leads to

$$\hat{\mathbf{a}}_{n+1} = c_1 \hat{\mathbf{u}}_{n+1} - \hat{\mathbf{a}}_n^* \quad \hat{\mathbf{a}}_n^* = c_1 \hat{\mathbf{u}}_n + c_2 \hat{\mathbf{v}}_n + c_3 \hat{\mathbf{a}}_n \quad (3.5)$$

$$\hat{\mathbf{v}}_{n+1} = \hat{\mathbf{v}}_n + (1 - \gamma)\Delta t \hat{\mathbf{a}}_n + \gamma \Delta t \hat{\mathbf{a}}_{n+1}, \quad \hat{\mathbf{v}}_n^* = c_4 \hat{\mathbf{u}}_n + c_5 \hat{\mathbf{v}}_n + c_6 \hat{\mathbf{a}}_n \quad (3.6)$$

where

$$c_1 = \frac{1}{\beta \Delta t^2} \quad c_2 = \frac{1}{\beta \Delta t} \quad c_3 = \frac{1 - 2\beta}{2\beta}$$

$$c_4 = \frac{\gamma}{\beta\Delta t} \quad c_5 = \frac{\gamma - \beta}{\beta} \quad c_6 = \frac{\Delta t(\gamma - 2\beta)}{2\beta}$$

where γ and β are stability parameters that originates from the trapezoidal rule. With the time approximation above and with dampening not included, the residual 3.1 can be expressed as

$$\tilde{\mathbf{R}} = c_1 \mathbf{M} \hat{\mathbf{u}} + \mathbf{F}_{int} - \mathbf{F}_{ext} - \mathbf{M}^n \mathbf{a}' \quad (3.7)$$

where the velocity and the acceleration increment has been replaced with

$$\mathbf{a}' = {}^n \mathbf{a}^* + d_1 {}^n \mathbf{v}^*. \quad (3.8)$$

Integrating this over Gauss-points and elements the result is

$${}^{n+1} \tilde{\mathbf{R}} = \sum_{Elements} \sum_{GP} \left(c_1 \rho \mathbf{N}^T \mathbf{N}^{n+1} \hat{\mathbf{u}} + \mathbf{B}({}^{n+1} \hat{\mathbf{u}})^{n+1} \mathbf{S} - \rho \mathbf{N}^T \mathbf{N}^n \mathbf{a}' \right) J^{iso} w_{weight} - \mathbf{F}_{ext}. \quad (3.9)$$

3.2 Non-linear solution procedure

To solve the non-linear equation in 3.7 consider a linearization of the virtual work in 2.48 in the form of a truncated Taylor expansion around the known state n where ${}^n \mathbf{u}$, ${}^n \mathbf{v}$ and ${}^n \mathbf{a}$ are known

$$\mathcal{V}(\mathbf{u} + d\mathbf{u}, \mathbf{v} + d\mathbf{v}, \delta\mathbf{u}) = \mathcal{V}(\mathbf{u}, \mathbf{v}, \mathbf{a}(\mathbf{v}), \delta\mathbf{u}) + d(\mathcal{V}(\mathbf{u}, \mathbf{v}, \mathbf{a}(\mathbf{v}), \delta\mathbf{u})) = 0. \quad (3.10)$$

Here it's assumed that the structure is in equilibrium in the new state and hence the incremental virtual work is equal to the former state like

$$d(\mathcal{V}(\mathbf{u}, \mathbf{v}, \mathbf{a}(\mathbf{v}), \delta\mathbf{u})) = -\mathcal{V}(\mathbf{u}, \mathbf{v}, \mathbf{a}(\mathbf{v}), \delta\mathbf{u}) \quad (3.11)$$

where the internal incremental virtual displacement is calculated as

$$d(\mathcal{V}(\mathbf{u}, \delta\mathbf{u})) = \left(\frac{\partial \mathcal{V}}{\partial \mathbf{u}} + \frac{\gamma}{\beta \Delta t} \frac{\partial \mathcal{V}}{\partial \mathbf{v}} + \frac{1}{\beta \Delta t^2} \frac{\partial \mathcal{V}}{\partial \mathbf{a}} \right) d\mathbf{u}. \quad (3.12)$$

In the above expression the incremental acceleration $d\mathbf{a}$ and the incremental velocity $d\mathbf{v}$ has been substituted according to 3.6 and 3.5.

An attempt is now made to factorize the equation in an expression including the incremental displacement as a factor, this can be seen in e.g. [7]. This forms the incremental virtual work as

$$d(\mathcal{V}(\mathbf{u}, \delta\mathbf{u})) = \delta\mathbf{a}\mathbf{K}d\mathbf{a}. \quad (3.13)$$

and finally 3.12 using 3.7 results in

$$\mathbf{K}d\mathbf{a} = -\tilde{\mathbf{R}} \quad (3.14)$$

If the dampening is neglected, the effective tangent stiffness matrix is express as

$$\mathbf{K} = c_1\mathbf{M} + \mathbf{K}_T \quad (3.15)$$

where the tangent stiffness matrix can be expressed as

$$\mathbf{K}_T = \int_{v_0} \mathbf{B}_0^T \mathbf{D} \mathbf{B}_0 dv^0 + \int_{v^0} \mathbf{H}_0^T \mathbf{R} \mathbf{H}_0 dv^0. \quad (3.16)$$

\mathbf{D} is the incremental relation between the second Piola-Kirchhoff stress tensor and the Green's strain and can be expressed as

$$d\mathbf{S}_\square = \mathbf{D} : d\mathbf{E}_\square \quad (3.17)$$

where the derivation of the algorithmic tangent stiffness can be seen in appendix C together with the \mathbf{H}_0 and \mathbf{R} matrices. The total stiffness matrix (3.15) and the internal force is in the FEM-program calculated on element level and than assembled into a global stiffness matrix, global force matrix respectively as

$$\mathbf{K} = \bigcup_{e=1}^{n_{elem}} \mathbf{K}^e \quad \mathbf{F}_{int} = \bigcup_{e=1}^{n_{elem}} \mathbf{F}_{int}^e \quad (3.18)$$

The structural problem in 3.14 is solved using a Newton-Raphson iteration scheme, see e.g. [7]. The use of isoparametric elements are used and integration is done using Gauss points see eg. [13].

3.3 Integration of Constitutive equations and the radial return method

To calculate the internal forces, the stresses need to be calculated in the new state and following, also the internal state variables. The evolution of the plastic flow, ie. the stresses and the internal state variables are given from the evolution laws and the yield function as in 2.36. Using the backward Euler method to integrate, the evolution equations become

$${}^1\mathbf{C} = {}^{n+1}\mathbf{F}({}^{n+1}\mathbf{G}^P - {}^n\mathbf{G}^P){}^{n+1}\mathbf{F}^T + 2\Delta\lambda\frac{1}{3}\text{tr}({}^{n+1}\bar{\mathbf{b}}^e){}^{n+1}\mathbf{n} \quad \text{flow rule} \quad (3.19)$$

$${}^{n+1}\alpha - {}^n\alpha = \Delta\lambda\sqrt{\frac{2}{3}} \quad \text{evolution for } \alpha \quad (3.20)$$

$${}^2C = f = \|\text{dev}({}^{n+1}\boldsymbol{\tau})\| - \sqrt{\frac{2}{3}}(K'({}^{n+1}\alpha, {}^{n+1}\theta) + \hat{y}({}^{n+1}\theta)) \quad \text{yield function} \quad (3.21)$$

$${}^3C = {}^n\theta - {}^{n+1}\theta - \frac{\eta}{\rho_0 c} {}^{n+1}\hat{\sigma}({}^{n+1}\theta)({}^{n+1}\alpha - {}^n\alpha) \quad \text{Heat equation} \quad (3.22)$$

where $\Delta\lambda = {}^{n+1}\lambda - {}^n\lambda$. $\mathbf{C} = [{}^1\mathbf{C}, {}^2C, {}^3C]$ is the local residual and this denoting is later used in the optimization section.

Define a trial elastic state, remembering $\text{dev}[\boldsymbol{\tau}] = \mu\text{dev}[\bar{\mathbf{b}}^e]$ from 2.26, as

$$\bar{\mathbf{b}}^{e,\text{trial}} := \bar{\mathbf{F}}^n \mathbf{G}^p \bar{\mathbf{F}}^{nT}, \quad (3.23)$$

$$\text{dev}[\boldsymbol{\tau}^{\text{trial}}] := \mu\text{dev}[\bar{\mathbf{b}}^{e,\text{trial}}], \quad (3.24)$$

$$f^{\text{trial}} := \|\text{dev}[\boldsymbol{\tau}^{\text{trial}}]\| - \sqrt{\frac{2}{3}}[\hat{K}'(\alpha_n, \theta) + \hat{y}(\theta)]. \quad (3.25)$$

$$\theta^{\text{trial}} = {}^n\theta \quad (3.26)$$

In this trial elastic state, the yield function indicates if the state is in the plastic region or not,

- $f^{\text{trial}} < 0$ - Elastic respons. Stresses and ISV are updated as $\text{dev}[\boldsymbol{\tau}^{\text{trial}}] = \text{dev}[\boldsymbol{\tau}^{\text{trial}}]$, ${}^{n+1}\mathbf{w} = \mathbf{w}^{\text{trial}}$, $\Delta\lambda = 0$
- $f^{\text{trial}} > 0$ - Plastic response, $\Delta\lambda > 0$

For plastic response, i.e. $f^{\text{trial}} > 0$ a way to calculate the plastic material behaviour is necessary. Calculating the trace of the flow rule in 3.19, it's concluded that

$$\text{tr}({}^{n+1}\bar{\mathbf{b}}^e) = \text{tr}(\bar{\mathbf{b}}^{e,\text{trial}}). \quad (3.27)$$

holds. The deviatoric part of the flow rule 3.19 yields

$$\text{dev}({}^{n+1}\boldsymbol{\tau}) = \text{dev}(\boldsymbol{\tau}^{\text{trial}}) - 2\mu\Delta\lambda \frac{1}{3} \text{tr}(\bar{\mathbf{b}}^{e,\text{trial}}) \underbrace{\frac{\text{dev}(\boldsymbol{\tau})}{\|\text{dev}\boldsymbol{\tau}\|}}_{\mathbf{n}} \quad (3.28)$$

The expression for the deviatoric part of the stress contains the unknown $\Delta\lambda$. To find this, insert 3.28 into the yield function 3.26 which is equal to zero when plastic deformation occurs

$$f := \|\text{dev}[\boldsymbol{\tau}^{\text{trial}}]\| - \sqrt{\frac{2}{3}}\mu \text{tr}(\bar{\mathbf{b}}^{e,\text{trial}})d\alpha - \sqrt{\frac{2}{3}}[\hat{K}'({}^{n+1}\alpha, {}^{n+1}\theta) + \hat{y}({}^{n+1}\theta)] = 0 \quad (3.29)$$

The yield function contains the unknown ${}^{n+1}\alpha$ and the temperature ${}^{n+1}\theta$ thus one variable needs to be eliminated. This is done by considering the heat equation in 3.22. With approximation for the mechanical work, the temperature can be expressed explicitly like a function of ${}^{n+1}\alpha$, ie. ${}^{n+1}\theta({}^{n+1}\alpha)$ and thus ${}^{n+1}\alpha$ can be solved for in the yield function with Newton-Raphson's algorithm see Appendix A.1. The resulting ${}^{n+1}\alpha$ is then inserted into the deviatoric part of the flow rule 3.28 and the stress is known.

To update the deviatoric part of $\bar{\mathbf{b}}^e$, the expression for the deviatoric stress 2.26 is used

$$\text{dev}[{}^{n+1}\bar{\mathbf{b}}^e] = \frac{1}{\mu} \text{dev}[{}^{n+1}\boldsymbol{\tau}]. \quad (3.30)$$

This, together with the volumetric part that is known from 3.27 is used when updating $\bar{\mathbf{b}}^e$.

Chapter 4

Optimization

In this work, the goal is to find the structure that absorbs as much energy as possible when loaded. The objective function is thus chosen as the discretized plastic work referring to 2.20

$$W^p = \sum_{n=1}^M \int_{\Omega_0} \sigma_y({}^{n+1}\alpha, {}^{n+1}\theta)({}^{n+1}\alpha - {}^n\alpha) dV \quad (4.1)$$

where n is the time steps t_n and M is the total number of time steps to reach the prescribed load. The optimization problem of the plastic work is written as

$$\mathcal{O} : \begin{cases} \min - W^p(\phi) = W^p({}^M\hat{\mathbf{w}}(\phi), {}^{M-1}\hat{\mathbf{w}}(\phi), \dots, {}^0\hat{\mathbf{w}}(\phi), \phi) \\ \text{s.t.} : g_V = \sum_{e=1}^{n_{elm}} \rho_0 V_{0e} c_{0e} - m \leq 0 \end{cases} \quad (4.2)$$

where the design variable $\phi(\mathbf{X}) = \phi_e$ is the density field which consists of the piece wise constant density ϕ_e that is constant in each element. $\hat{\mathbf{w}}$ is provided by solving the residuals

$$\tilde{\mathbf{R}}({}^n\hat{\mathbf{u}}(\phi), {}^{n-1}\hat{\mathbf{u}}(\phi), {}^n\hat{\mathbf{w}}(\phi), {}^{n-1}\hat{\mathbf{w}}(\phi), {}^n\phi) = 0, \quad n = 1, 2, \dots, M \quad (4.3)$$

$$\mathbf{C}({}^n\hat{\mathbf{u}}(\phi), {}^{n-1}\hat{\mathbf{u}}(\phi), {}^n\hat{\mathbf{w}}(\phi), {}^{n-1}\hat{\mathbf{w}}(\phi), {}^n\phi) = 0, \quad n = 1, 2, \dots, M \quad (4.4)$$

remembering from 3.19 and 3.21 \mathbf{C} being the local residual. The formulation in 4.2 is called a nested formulation since the equilibrium constraint have been written as a function of the design variables. This problem can be solved by several optimization procedures where a breakdown consists of gradient based optimizers and non gradient based optimizers such as the response surface-based method as in e.g. [9]. For problems with large degrees of freedom it is known that the response surface-based methods

become inefficient, and a gradient based optimization technique is therefore chosen. The problem at hand is non-convex and since this is a basic requirement for use of convex programming (see eg. [1]) a convex approximation is therefore required. The method used is the method of moving asymptotes (MMA), cf. [16] where the gradients of the constraints and the objective function is used to make the problem convex.

4.1 Material interpolation and regularization

In order to make the density either take values 1 or 0, a non-linear interpolation is introduced for the material parameters in the constitutive model. This is to make intermediate designs further from optimum, i.e. penalize designs with lots of element densities between 0 (void) and 1 (full material). The RAMP scheme has been chosen according to [15] and, for example, the shear modulus is penalized as

$$\kappa(c) = \kappa_0 + \frac{\rho}{1 + q(1 - \rho)}(\kappa_1 - \kappa_0) \quad (4.5)$$

where the ρ is the physical volume fraction field, κ_1 represents the bulk modulus at full material, κ_0 is a value close to zero, in order to avoid numerical problems. To control the level of penalization, the parameter q is introduced. In the same way as for κ , μ , H , σ_{y_0} and σ_{y_∞} are also penalized using RAMP. The mass matrix is also penalized like

$$\mathbf{M} = \int_{\Omega_0} \rho_0(\rho) \mathbf{N}^T \mathbf{N} dV \quad (4.6)$$

To obtain a mesh independent solution and to avoid checkerboard patterns see e.g.[1] filters are introduced. In addition, to obtain a clear distinction between void material phase and full material, a Heaviside thresholding technique is used. The continuous density variable $\tilde{\rho} \in [0 \ 1]$ is introduced to describe the full material, $\tilde{\rho} = 1$, and the void phase, $\tilde{\rho} = 0$. The field of $\tilde{\rho}$ is given from the design variable ϕ_e via the Helmholtz's equation see [10]

$$-R^2 \Delta_0 \tilde{\rho} + \tilde{\rho} = \phi \quad (4.7)$$

where Δ_0 is the Laplacian, and R is the filter radius. In order to remove intermediate designs a Heaviside thresholding filter is introduced, see e.g. [2]

$$\rho = \frac{\tanh(\beta_H \omega_H) + \tanh(\beta_H (\tilde{\rho} - \omega_H))}{\tanh(\beta_H \omega_H) + \tanh(\beta_H (1 - \omega_H))} \quad (4.8)$$

where β_H and ω_H are parameters describing the steepness of the Heaviside function.

4.2 Sensitivity analysis

The gradients of a functional are called sensitivities. Remember that in the case of plasticity, the deformation is path dependent and the computation split up to into time steps. When optimizing the structure, the entire path needs to be included and following, the derivatives in all time steps need to be calculated. The sensitivities can be calculated either numerical or analytically, where the latter is preferable for accuracy. When calculating analytical, the direct method can be used if the number of design variables are small however, for larger systems the adjoint method for coupled transient problems presented in [11] is significantly more computational efficient. The main features of this method is to introduce an augmented objective function by substituting a two terms consisting of a product of an adjoint variable and the discretized mechanical balance law 4.3 an an adjoint variable and the discretized evolution laws 4.4. By doing this, the implicit response sensitivities can be entirely eliminated from the expression of the sensitivities.

4.2.1 Numerical differentiation

Using the forward difference method, the sensitivity can be calculated

$$\frac{\partial W_p(\phi)}{\partial \phi_j} \approx \frac{W_p(\phi + h e_j) - W_p(\phi)}{h} \quad (4.9)$$

where $e_j = 1$ for index j on the design variable and $e_j = 0$ otherwise. This is to be done for each design variable.

4.2.2 Adjoint method

The sensitivities of the objective function with respect to the design variable are

$$\frac{DW^p}{D\phi_e} = \sum_{n=1}^M \left(\frac{\partial W^p}{\partial^n \mathbf{w}} \frac{D^n \mathbf{w}}{D\phi_e} \right) + \frac{\partial W^p}{\partial \phi_e} \quad (4.10)$$

The implicit derivatives $D^n \mathbf{w} / D\phi_e$ are computationally costly to calculate. These can be eliminated using the adjoint method. Introduce an augmented objective function

\hat{W}^p with the adjoint variables $\boldsymbol{\lambda}, \gamma, \boldsymbol{\lambda}_{\hat{\mathbf{u}}}, \boldsymbol{\lambda}_{\hat{\mathbf{v}}}$

$$\begin{aligned} \hat{W}^p = & W^p(M \hat{\mathbf{w}}(\boldsymbol{\phi}), M-1 \hat{\mathbf{w}}(\boldsymbol{\phi}), \dots, {}^0 \hat{\mathbf{w}}(\boldsymbol{\phi})) \\ & - \sum_{n=1}^M {}^{M-n+1} \boldsymbol{\lambda} \hat{\mathbf{R}}({}^n \hat{\mathbf{u}}(\boldsymbol{\phi}), {}^n \mathbf{w}(\boldsymbol{\phi}), \boldsymbol{\phi}) \\ & - \sum_{n=1}^N {}^{M-n+1} \gamma \mathbf{C}({}^n \hat{\mathbf{u}}(\boldsymbol{\phi}), {}^{n-1} \hat{\mathbf{u}}(\boldsymbol{\phi}), {}^n \mathbf{w}(\boldsymbol{\phi}), {}^{n-1} \mathbf{w}(\boldsymbol{\phi}), \boldsymbol{\phi}) \\ & - \sum_{n=1}^N {}^{M-n+1} \boldsymbol{\lambda}_{\hat{\mathbf{u}}} \left({}^{n-1} \hat{\mathbf{u}}(\boldsymbol{\phi}) + \Delta^n t^{n-1} \hat{\mathbf{v}}(\boldsymbol{\phi}) + \frac{1-2\beta}{2} \Delta^n t^{2n-1} \hat{\mathbf{a}}(\boldsymbol{\phi}) + \beta \Delta^n t^2 \hat{\mathbf{a}}(\boldsymbol{\phi}) - {}^n \hat{\mathbf{u}}(\boldsymbol{\phi}) \right) \\ & - \sum_{n=1}^N {}^{M-n+1} \boldsymbol{\lambda}_{\hat{\mathbf{v}}} \left({}^{n-1} \hat{\mathbf{v}}(\boldsymbol{\phi}) + (1-\gamma) \Delta^n t^{n-1} \hat{\mathbf{a}}(\boldsymbol{\phi}) + \gamma \Delta^n t \hat{\mathbf{a}}(\boldsymbol{\phi}) - {}^n \hat{\mathbf{v}}(\boldsymbol{\phi}) \right) \end{aligned}$$

Because the residual of the mechanical balance law 4.3 and the evolution equations 4.4 are equal to zero and 3.5 and 3.6 hold for $\hat{\mathbf{u}}$ and $\hat{\mathbf{v}}$, the augmented objective function is equal to the normal objective function i.e. $\hat{W}^p = W^p$. Note also that the derivative of the augmented objective function equals the objective function, i.e. $DW^p/D\phi_e = D\hat{W}^p/D\phi_e$ since the derivative of 4.3, 4.4 and the third and fourth term 3.5 and 3.6 being equal to zero. Differentiation of the augmented objective function with respect to the design variable leads to the expression

$$\begin{aligned} \frac{D\hat{W}^p}{D\phi_e} = & \frac{\partial W^p}{\partial \phi_e} + \sum_{n=1}^M \left(\frac{\partial W^p}{\partial^n \mathbf{w}} \frac{D^n \mathbf{w}}{D\phi_e} \right) \\ & - \sum_{n=1}^M ({}^{M-n+1} \boldsymbol{\lambda})^T \left[\frac{\partial^n \hat{\mathbf{R}}}{\partial^n \hat{\mathbf{u}}} \frac{D^n \hat{\mathbf{u}}}{D\phi_e} + \frac{\partial^n \hat{\mathbf{R}}}{\partial^n \mathbf{w}} \frac{D^n \mathbf{w}}{D\phi_e} + \frac{\partial^n \hat{\mathbf{R}}}{\partial \phi_e} \right] \\ & - \sum_{n=1}^M ({}^{M-n+1} \gamma)^T \left[\frac{\partial^n \mathbf{C}}{\partial^n \hat{\mathbf{u}}} \frac{D^{n-1} \hat{\mathbf{u}}}{D\phi_e} + \Delta t_n \frac{D^{n-1} \hat{\mathbf{v}}}{D\phi_e} + \frac{1-2\beta}{2} \Delta^n t^2 \frac{D^{n-1} \hat{\mathbf{a}}}{D\phi_e} + \beta \Delta^n t^2 \frac{D \hat{\mathbf{a}}}{D\phi_e} \right. \\ & \quad \left. + \frac{\partial^n \mathbf{C}}{\partial^n \mathbf{w}} \frac{D^n \mathbf{w}}{D\phi_e} + \frac{\partial^n \mathbf{C}}{\partial^{n-1} \hat{\mathbf{u}}} \frac{D^{n-1} \hat{\mathbf{u}}}{D\phi_e} + \frac{\partial^n \mathbf{C}}{\partial^{n-1} \mathbf{w}} \frac{D^{n-1} \mathbf{w}}{D\phi_e} + \frac{\partial^n \mathbf{C}}{\partial \phi_e} \right] \\ & - \sum_{n=1}^M ({}^{M-n+1} \boldsymbol{\lambda}_{\hat{\mathbf{u}}})^T \left[\frac{D^{n-1} \hat{\mathbf{u}}}{D\phi_e} + \Delta t_n \frac{D^{n-1} \hat{\mathbf{v}}}{D^{n-1} \hat{\phi}_e} + \Delta t_n \frac{D^{n-1} \hat{\mathbf{v}}}{\phi_e} + \frac{1-2\beta}{2} \Delta^n t^2 \frac{D \hat{\mathbf{a}}}{D\phi_e} - \frac{D \hat{\mathbf{u}}}{D\phi_e} \right] \\ & - \sum_{n=1}^M ({}^{M-n+1} \boldsymbol{\lambda}_{\hat{\mathbf{v}}})^T \left[\frac{D^{n-1} \hat{\mathbf{v}}}{D\phi_e} + (1-\gamma) \Delta t_n \frac{D^n \hat{\mathbf{a}}}{D\phi_e} + \gamma \Delta t_n \frac{D^n \hat{\mathbf{a}}}{D\phi_e} - \frac{D^n \hat{\mathbf{v}}}{\phi_e} \right]. \end{aligned} \tag{4.11}$$

This can be split into an explicit term $D\hat{W}_E^p/D\phi_e$ and an implicit term $D\hat{W}_I^p/D\phi_e$ where the implicit term contains all the implicit derivatives that will be eliminated

$$\frac{D\hat{W}^p}{D\phi_e} = \frac{D\hat{W}_E^p}{D\phi_e} + \frac{D\hat{W}_I^p}{D\phi_e}, \quad (4.12)$$

$$\frac{D\hat{W}_I^p}{D\phi_e} = \sum_{n=1}^M \left(\frac{D\hat{W}_I^p}{D\phi_e} \right)_{\lambda} + \sum_{n=1}^M \left(\frac{D\hat{W}_I^p}{D\phi_e} \right)_{\lambda_{\hat{u}}} + \sum_{n=1}^M \left(\frac{D\hat{W}_I^p}{D\phi_e} \right)_{\lambda_{\hat{v}}} + \sum_{n=1}^M \left(\frac{D\hat{W}_I^p}{D\phi_e} \right)_{\gamma}, \quad (4.13)$$

$$\begin{aligned} \frac{D\hat{W}_E^p}{D\phi_e} &= \frac{\partial W^p}{\partial \phi_e} - \sum_{n=1}^M \left(\boldsymbol{\lambda}^{(M-n+1)} \right)^T \frac{\partial^n \tilde{\mathbf{R}}}{\partial \phi_e^n} - \sum_{n=1}^M \left(\boldsymbol{\gamma}^{(M-n+1)} \right)^T \frac{\partial^n \mathbf{C}}{\partial \phi_e^n} \\ &\quad - \left(\frac{D^0 \hat{\mathbf{u}}}{D\phi_e} \right)^T \left[\frac{1-2\beta}{2} \Delta t_1^2 \left(\frac{\partial^1 \mathbf{C}}{\partial^1 \hat{\mathbf{u}}} \right)^T {}^M \boldsymbol{\gamma} + \frac{1-2\beta}{2} \Delta t_1^{2M} \boldsymbol{\lambda}_{\hat{u}} + (1-\gamma) \Delta t_1^M \boldsymbol{\lambda}_{\hat{v}} \right] \\ &\quad - \left(\frac{D^0 \hat{\mathbf{v}}}{D\phi_e} \right)^T \left[\Delta t_1 \left(\frac{\partial^1 \mathbf{C}}{\partial^1 \hat{\mathbf{u}}} \right)^T {}^M \boldsymbol{\gamma} + \Delta t_1^M \boldsymbol{\lambda}_{\hat{u}} + {}^M \boldsymbol{\lambda}_{\mathbf{v}} \right] \\ &\quad - \left(\frac{D^0 \hat{\mathbf{u}}}{D\phi_e} \right)^T \left[\left(\frac{\partial^1 \mathbf{C}}{\partial^1 \hat{\mathbf{u}}} \right)^T {}^M \boldsymbol{\gamma} + \left(\frac{\partial^1 \mathbf{C}}{\partial^0 \hat{\mathbf{u}}} \right)^T {}^M \boldsymbol{\gamma} - {}^M \boldsymbol{\lambda}_{\mathbf{u}} \right] - \left(\frac{D^0 \mathbf{w}}{D\phi_e} \right)^T \left(\frac{\partial^1 \mathbf{C}}{\partial^0 \mathbf{w}} \right)^T {}^M \boldsymbol{\gamma} \end{aligned} \quad (4.14)$$

where the implicit part is written in a compact form where the subindex λ represent the implicit contribution from the third term in 4.11, the $\lambda_{\hat{u}}$ represent the contribution from the fourth term etc. Rearranging 4.11 in order to get the implicit derivatives as

factors to the terms in an expression the result is

$$\begin{aligned}
\frac{D\hat{W}_I^p}{D\phi_e} = & - \sum_{n=1}^{M-1} \left(\frac{\partial D^n \hat{\mathbf{a}}}{\partial D\phi_e} \right)^T \left\{ \beta \Delta t_n^2 \left(\frac{\partial^n \mathbf{C}}{\partial^n \hat{\mathbf{u}}} \right)^T \gamma^{M-n+1} + \beta \Delta t_n^{2(M-n+1)} \boldsymbol{\lambda}_{\hat{\mathbf{u}}} + \gamma \Delta t_n^{M-n+1} \boldsymbol{\lambda}_{\hat{\mathbf{v}}} \right. \\
& \left. + \frac{1-2\beta}{2} \Delta t_{n+1}^2 \left[\left(\frac{\partial^{n+1} \mathbf{C}}{\partial^{n+1} \hat{\mathbf{u}}} \right)^T M^{-n} \gamma + \boldsymbol{\lambda}_{\hat{\mathbf{u}}} \right] + (1-\gamma) \Delta t_{n+1}^{M-n} \boldsymbol{\lambda}_{\hat{\mathbf{v}}} \right\} \\
& - \sum_{n=1}^{M-1} \left(\frac{\partial D^n \hat{\mathbf{v}}}{\partial D\phi_e} \right)^T \left\{ \Delta t_{n+1} \left(\frac{\partial^{n+1} \mathbf{C}}{\partial^{n+1} \hat{\mathbf{u}}} \right)^{M-1} \gamma + \Delta t_{n+1}^{M-n} \boldsymbol{\lambda}_{\hat{\mathbf{u}}} + M^{-n+1} \boldsymbol{\lambda}_{\hat{\mathbf{v}}} - M^{-n} \boldsymbol{\lambda}_{\hat{\mathbf{v}}} \right\} \\
& - \sum_{n=1}^{M-1} \left(\frac{\partial D^n \hat{\mathbf{u}}}{\partial D\phi_e} \right)^T \left\{ \left(\frac{\partial^n \tilde{\mathbf{R}}}{\partial^n \hat{\mathbf{u}}} \right)^T M^{-n+1} \boldsymbol{\lambda} + M^{-n} \boldsymbol{\lambda}_{\hat{\mathbf{u}}} + M^{-n+1} \boldsymbol{\lambda}_{\hat{\mathbf{u}}} \right. \\
& \left. + \left[\left(\frac{\partial^{n+1} \mathbf{C}}{\partial^{n+1} \hat{\mathbf{u}}} \right)^T + \left(\frac{\partial^{n+1} \mathbf{C}}{\partial^n \hat{\mathbf{u}}} \right)^T \right] M^{-n} \gamma \right\} \\
& - \sum_{n=1}^{M-1} \left(\frac{D^n \mathbf{w}}{D\phi_e} \right) \left\{ - \left(\frac{\partial W^p}{\partial^n \mathbf{w}} \right)^T + \left(\frac{\partial^n \tilde{\mathbf{R}}}{\partial^n \mathbf{w}} \right)^T M^{-n+1} \boldsymbol{\lambda} + \left(\frac{\partial^n \mathbf{C}}{\partial^n \mathbf{w}} \right)^T M^{-n+1} \gamma \right. \\
& \left. + \left(\frac{\partial^{n+1} \mathbf{C}}{\partial^n \mathbf{w}} \right)^T M^{-n} \gamma \right\} \\
& - \left(\frac{D^M \hat{\mathbf{a}}}{D\phi_e} \right)^T \left\{ \beta \Delta t_M^2 \left(\frac{\partial^M \mathbf{C}}{\partial^M \hat{\mathbf{u}}} \right)^T \boldsymbol{\lambda} + \beta \Delta t_M^{2M} \boldsymbol{\lambda}_{\hat{\mathbf{v}}} \right\} \\
& - \left(\frac{D^M \hat{\mathbf{v}}}{D\phi_e} \right)^T \left\{ - \boldsymbol{\lambda}_{\hat{\mathbf{v}}} \right\} \\
& - \left(\frac{D^M \hat{\mathbf{u}}}{D\phi_e} \right)^T \left\{ \left(\frac{\partial^M \tilde{\mathbf{R}}}{\partial^M \hat{\mathbf{u}}} \right)^T \boldsymbol{\lambda} - \boldsymbol{\lambda}_{\hat{\mathbf{u}}} \right\} \\
& - \left(\frac{D^M \hat{\mathbf{w}}}{D\phi_e} \right)^T \left\{ - \left(\frac{\partial W^p}{\partial^M \mathbf{w}} \right)^T + \left(\frac{\partial^M \tilde{\mathbf{R}}}{\partial^M \mathbf{w}} \right)^T \boldsymbol{\lambda} + \left(\frac{\partial^M \mathbf{C}}{\partial^M \mathbf{w}} \right)^T \boldsymbol{\lambda} \right\}. \tag{4.15}
\end{aligned}$$

The task is now to eliminate the implicit derivatives by setting the factor with the brackets to zero. Starting with the last terms in step N , more precisely $D\hat{\mathbf{u}}^N/D\phi_e$ and $D\hat{\mathbf{v}}^N/D\phi_e$ the brackets are set to zero like

$${}^1 \boldsymbol{\lambda}_{\hat{\mathbf{u}}} = \left(\frac{\partial^N \tilde{\mathbf{R}}}{\partial^N \hat{\mathbf{u}}} \right)^T \boldsymbol{\lambda}, \tag{4.16}$$

$${}^1 \boldsymbol{\lambda}_{\hat{\mathbf{v}}} = \mathbf{0}. \tag{4.17}$$

Continuing at the last step, $D^N \hat{\mathbf{a}}/D\phi_e$ and ${}^N D\mathbf{w}/D\phi_e$ are eliminated by solving the system of equations for ${}^1\boldsymbol{\lambda}$ and ${}^1\boldsymbol{\gamma}$ like

$$\begin{cases} \beta \Delta t_M^2 \left(\frac{\partial^N \mathbf{C}}{\partial^N \mathbf{w}} \right) {}^1\boldsymbol{\gamma} = [\beta \Delta t_N^2 {}^1\boldsymbol{\lambda}_{\hat{\mathbf{u}}} + \gamma \Delta t_N \boldsymbol{\lambda}_{\hat{\mathbf{v}}}] \\ \left(\frac{\partial^N \tilde{\mathbf{R}}}{\partial^N \mathbf{w}} \right)^T {}^1\boldsymbol{\lambda} + \left(\frac{\partial^N \mathbf{C}}{\partial^N \mathbf{w}} \right) {}^1\boldsymbol{\gamma} = \left(\frac{\partial W^p}{\partial^N \mathbf{w}} \right)^T \end{cases} \quad (4.18)$$

rearranging, the first equation yields that ${}^1\boldsymbol{\lambda}$ can be expressed explicitly

$$\begin{cases} \beta \Delta^N t^2 ({}^N \tilde{\mathbf{K}})^T {}^1\boldsymbol{\lambda} = \beta \Delta t_M^2 \overbrace{\left[\left(\frac{\partial W^p}{\partial^N \mathbf{w}} \right) \left(\frac{\partial^N \mathbf{C}}{\partial^N \mathbf{w}} \right)^{-1} \left(\frac{\partial^N \mathbf{C}}{\partial^N \hat{\mathbf{u}}} \right) \right]}^{N\Gamma} \\ \left(\frac{\partial^N \mathbf{C}}{\partial^N \mathbf{w}} \right) {}^1\boldsymbol{\gamma} = \left[\left(\frac{\partial W^p}{\partial^N \mathbf{w}} \right)^T - \left(\frac{\partial^N \tilde{\mathbf{R}}}{\partial^N \mathbf{w}} \right)^T {}^1\boldsymbol{\lambda} \right] \end{cases} \quad (4.19)$$

where Γ is called the pseudo load vector and $\tilde{\mathbf{K}}$ is the effective tangent stiffness matrix. After ${}^1\boldsymbol{\lambda}$ has been calculated, insert this in the second equation in 4.19 to get ${}^1\boldsymbol{\gamma}$. Now the implicit derivatives in the last step has been eliminated, and the implicit derivatives in the remaining time steps

$$\frac{D^{M-n+1} \hat{\mathbf{u}}}{D\phi_e}, \quad \frac{D^{M-n+1} \hat{\mathbf{v}}}{D\phi_e}, \quad \frac{D^{M-n+1} \hat{\mathbf{a}}}{D\phi_e}, \quad \frac{D^{M-n+1} \mathbf{w}}{D\phi_e} \quad (4.20)$$

are to be dealt with. Starting with the first two terms they are eliminated by solving

$$\begin{cases} \boldsymbol{\lambda}_{\hat{\mathbf{u}}} = \left(\frac{\partial^{M-n+1} \tilde{\mathbf{R}}}{\partial^{M-n+1} \hat{\mathbf{u}}} \right)^T \boldsymbol{\lambda} + \left(\frac{\partial^{M-n+2} \mathbf{C}}{\partial^{M-n+2} \hat{\mathbf{u}}} \right)^T {}^{n-1}\boldsymbol{\gamma} + \left(\frac{\partial^{M-n+2} \mathbf{C}}{\partial^{M-n+1} \hat{\mathbf{u}}} \right)^T {}^{n-1}\boldsymbol{\gamma} + {}^{n-1}\boldsymbol{\lambda}_{\hat{\mathbf{u}}}, \\ \boldsymbol{\lambda}_{\hat{\mathbf{v}}} = - \left(\frac{\partial W^p}{\partial^{M-n+1} \hat{\mathbf{v}}} \right)^T + \Delta t_{N-n+2} \left(\frac{\partial^{N-n+2} \mathbf{C}}{\partial^{N-n+2} \hat{\mathbf{u}}} \right)^T {}^{n-1}\boldsymbol{\gamma} + \Delta t_{N-n+2} {}^{n-1}\boldsymbol{\lambda}_{\hat{\mathbf{u}}} + {}^{n-1}\boldsymbol{\lambda}_{\hat{\mathbf{v}}} \end{cases} \quad (4.21)$$

and proceeding, the last two terms are eliminated in similar fashion

$$\left\{ \begin{aligned} \beta \Delta t_{N-n+1}^2 \left(\frac{\partial^{M-n+1} \mathbf{C}}{\partial^{M-n+1} \hat{\mathbf{u}}} \right)^T {}^n \boldsymbol{\gamma} &= - \left[\frac{1-2\beta}{2} \Delta t_{N-n+2} \left\{ \left(\frac{\partial^{N-n+2} \mathbf{C}}{\partial^{N-n+2} \hat{\mathbf{u}}} \right)^T {}^{n-1} \boldsymbol{\gamma} + {}^{n-1} \boldsymbol{\lambda}_{\hat{\mathbf{u}}} \right\} \right. \\ &\quad \left. + \beta \Delta t_{N-n+1}^2 {}^n \boldsymbol{\lambda}_{\hat{\mathbf{u}}} + (1-\gamma) \Delta t_{N-n+2}^{n-1} \boldsymbol{\lambda}_{\hat{\mathbf{v}}} + \gamma \Delta t_{N-n+1} {}^n \boldsymbol{\lambda}_{\hat{\mathbf{v}}} \right], \\ \left(\frac{\partial^{M-n+1} \tilde{\mathbf{R}}}{\partial^{M-n+1} \mathbf{w}} \right)^T {}^n \boldsymbol{\lambda} + \left(\frac{\partial^{M-n+1} \mathbf{C}}{\partial^{M-n+1} \mathbf{w}} \right)^T {}^n \boldsymbol{\gamma} &= - \left[- \left(\frac{\partial W^p}{\partial^{M-n+1} \mathbf{w}} \right)^T + \left(\frac{\partial^{M-n+2} \mathbf{C}}{\partial^{M-n+2} \mathbf{w}} \right)^T {}^{n-1} \boldsymbol{\gamma} \right] \end{aligned} \right. \quad (4.22)$$

which can be rearranged to

$$\left\{ \begin{aligned} \left({}^{N-n+1} \tilde{\mathbf{K}} \right)^T \boldsymbol{\lambda} &= - (\beta \Delta t_{N-n+1}^2)^{-1} {}^{N-n+1} \boldsymbol{\Gamma}(\boldsymbol{\lambda}_{\hat{\mathbf{u}}}, \boldsymbol{\lambda}_{\hat{\mathbf{v}}}) \\ \left(\frac{\partial^{M-n+1} \mathbf{C}}{\partial^{M-n+1} \mathbf{w}} \right)^T {}^n \boldsymbol{\gamma} &= - \left[- \left(\frac{\partial W^p}{\partial^{M-n+1} \mathbf{w}} \right)^T + \left(\frac{\partial^{M-n+2} \mathbf{C}}{\partial^{M-n+2} \mathbf{w}} \right)^T {}^{n-1} \boldsymbol{\gamma} \left(\frac{\partial^{M-n+1} \tilde{\mathbf{R}}}{\partial^{M-n+1} \mathbf{w}} \right)^T {}^n \boldsymbol{\lambda} \right]. \end{aligned} \right. \quad (4.23)$$

with the pseudoload vector

$$\begin{aligned} {}^{N-n+1} \boldsymbol{\Gamma}(\boldsymbol{\lambda}_{\hat{\mathbf{u}}}, \boldsymbol{\lambda}_{\hat{\mathbf{v}}}) &= - \left[\frac{1-2\beta}{2} \Delta t_{N-n+2} \left(\frac{\partial^{N-n+2} \mathbf{C}}{\partial^{N-n+2} \hat{\mathbf{u}}} \right)^T {}^{n-1} \boldsymbol{\gamma} \right. \\ &\quad \left. + \left(\frac{1-2\beta}{2} \Delta t_{M-n+2}^2 + \beta \Delta t_{N-n+1}^2 \right) {}^{n-1} \boldsymbol{\lambda}_{\hat{\mathbf{u}}} + (1-\gamma) \Delta t_{N-n+2} {}^{n-1} \boldsymbol{\lambda}_{\hat{\mathbf{v}}} + \gamma \Delta t_{M-n+1} {}^n \boldsymbol{\lambda}_{\hat{\mathbf{v}}} \right] \\ &\quad + \beta \Delta t_{M-n+1}^2 \left(\left\{ \left[\left(\frac{\partial^{M-n+2} \mathbf{C}}{\partial^{M-n+2} \mathbf{w}} \right) \left(\frac{\partial^{M-n+1} \mathbf{C}}{\partial^{M-n+1} \mathbf{w}} \right)^{-1} \left(\frac{\partial^{M-n+2} \mathbf{C}}{\partial^{M-n+1} \mathbf{w}} \right) \right]^T + \left(\frac{\partial^{M-n+2} \mathbf{C}}{\partial^{M-n+2} \mathbf{w}} \right)^T \right. \right. \\ &\quad \left. \left. + \left(\frac{\partial^{M-n+2} \mathbf{C}}{\partial^{M-n+1} \mathbf{w}} \right) \right\} {}^{n-1} \boldsymbol{\gamma} - \left[\left(\frac{\partial W^p}{\partial^{M-n+1} \mathbf{w}} \right) \left(\frac{\partial^{M-n+1} \mathbf{C}}{\partial^{M-n+1} \mathbf{w}} \right)^{-1} \left(\frac{\partial^{M-n+1} \mathbf{C}}{\partial^{M-n+1} \hat{\mathbf{u}}} \right) \right]^T \right) \end{aligned} \quad (4.24)$$

All the implicit terms are now eliminated so that $D\hat{W}_I^p/D\phi_e = 0$ and thus the only non zero term is the explicit term 4.14, i.e.

$$\frac{D\hat{W}^p}{D\phi_e} = \frac{D\hat{W}_E^p}{D\phi_e} \quad (4.25)$$

4.3 Sensitivities of large strain thermoplasticity

In the previous section the adjoint method was explained. All the necessary derivatives in the section, i.e. in 4.15 are here derived based on [6] but modified to fit the thermomechanical model. The outer residual is repeated here as

$${}^{n+1}\mathbf{R} = \sum_{Elements} \sum_{GP} \left(c_1 \rho_0(\rho) \mathbf{N}^T \mathbf{N}^{n+1} \hat{\mathbf{u}} + \mathbf{B}({}^{n+1}\hat{\mathbf{u}})^{n+1} \mathbf{S} - \rho \mathbf{N}^T \mathbf{N}^n \mathbf{a}' \right) J^{iso} w_{weight} - \mathbf{F}_{ext}. \quad (4.26)$$

When differentiating, the external force is independent of the state variables and the displacements, along with \mathbf{a}' that is known from the previous step. In the following section the internal force will be differentiated followed by the first term in the residual containing the mass matrix. The outer residual and the local residual are tensors that are quite cumbersome to express in matrix format, therefore the tensor notation explained in eg. [4] is utilized. Inserting $\mathbf{b}^e = \mathbf{F} \mathbf{G}^p \mathbf{F}^T$ from 2.3 in the flow rule, the local residual $\mathbf{C} = [{}^1\mathbf{C}, {}^2\mathbf{C}, {}^3\mathbf{C}]$ from 3.19 - 3.22 formulated for plasticity, elasticity respectively is in index notation

If plastic response

$${}^{n+1}\mathbf{C} = \begin{cases} {}^{n+1}({}^1\mathbf{C}_{ij}) = {}^{n+1} \bar{f}_{ik} \bar{b}_{kl}^{e} {}^{n+1} \bar{f}_{jl} - {}^{n+1} \bar{b}_{ij}^e - \sqrt{\frac{2}{3}} \Delta \alpha^{n+1} \bar{b}_{tt}^{e} {}^{n+1} n_{ij} & \text{flow rule} \\ {}^{n+1}({}^2\mathbf{C}) = \mu \sqrt{{}^{n+1} d_{xy} {}^{n+1} d_{xy}} - \sqrt{\frac{2}{3}} (K'({}^{n+1} \alpha, {}^{n+1} \theta) + \hat{\sigma}_y({}^{n+1} \theta)) & \text{yield function} \\ {}^{n+1}({}^3\mathbf{C}) = {}^n \theta - {}^{n+1} \theta + \frac{\eta}{\rho_0 c} {}^{n+1} \hat{\sigma}({}^{n+1} \theta) ({}^{n+1} \alpha - {}^n \alpha) & \text{Heat equation} \end{cases}$$

$${}^{n+1}\mathbf{w} = \begin{cases} {}^{n+1} \bar{b}_{ij}^e \\ {}^{n+1} \alpha \\ {}^{n+1} \theta \end{cases} \quad (4.27)$$

If elastic response

$${}^{n+1}\mathbf{C} = \begin{cases} {}^{n+1}({}^1\mathbf{C}_{ij}) = {}^{n+1} \bar{f}_{ik} \bar{b}_{kl}^{e} {}^{n+1} \bar{f}_{jl} - {}^{n+1} \bar{b}_{ij}^e & \text{flow rule} \\ {}^{n+1}\mathbf{w} = \begin{cases} {}^{n+1} \bar{b}_{ij}^e \end{cases} & \end{cases} \quad (4.28)$$

where the relative deformation gradient is defined as $f_{ij} := {}^{n+1}F_{ik}^{-1n}F_{kj}^{-1}$, and it's volume preserving variation as $\bar{f}_{ij} := {}^{n+1}\bar{F}_{ik}^{-1n}\bar{F}_{kj}^{-1}$. The deviatoric part of s_{ij} in index notation has been introduced as d_{ij} .

4.3.1 Derivatives of outer residual

The outer residual in 3.9 can be rewritten by replacing the second Piola-Kirchhoff with the Kirchhoff stress as $s_{ij} = F_{is}\tau_{ts}F_{jt}$ which results in

$${}^{n+1}(F_{int})^\gamma = \sum_{Elements} \sum_{GP} B_{ij}^\gamma ({}^{n+1}\hat{u}^\beta) {}^{n+1}F_{is}^{-1n+1}\tau_{ts} {}^{n+1}F_{jt}^{-1} J^{iso} w_{weight}. \quad (4.29)$$

The superscript in Greek letters like γ, β in 4.29 is the degree of freedom for one element as this is assembled into the global system see eg. [13]. α is also used as index here and is not to be confused with the internal variable α .

Beginning with the outer residual, the derivatives with respect to the current time step $n + 1$ are here presented briefly. First, the derivative with respect to the displacement is considered i.e.

$$\frac{\partial {}^{n+1}(F_{int})^\gamma}{\partial {}^{n+1}\hat{u}^\alpha} = \left(\frac{\partial B_{ij}^\gamma ({}^{n+1}\hat{u}^\beta)}{\partial {}^{n+1}\hat{u}^\alpha} {}^{n+1}F_{is}^{-1n+1}\tau_{st} {}^{n+1}F_{jt}^{-1} \right. \quad (4.30)$$

$$+ B_{ij}^\gamma ({}^{n+1}\hat{u}^\beta) \frac{\partial {}^{n+1}F_{is}^{-1n+1}\tau_{st} {}^{n+1}F_{jt}^{-1}}{\partial {}^{n+1}\hat{u}^\alpha} \quad (4.31)$$

$$+ B_{ij}^\gamma (\hat{u}^\beta) {}^{n+1}F_{is}^{-1} \frac{\partial {}^{n+1}\tau_{st} {}^{n+1}F_{jt}^{-1}}{\partial {}^{n+1}\hat{u}^\alpha} \quad (4.32)$$

$$+ B_{ij}^\gamma ({}^{n+1}\hat{u}^\beta) {}^{n+1}F_{is}^{-1n+1}\tau_{st} \frac{\partial {}^{n+1}F_{jt}^{-1}}{\partial {}^{n+1}\hat{u}^\alpha} \Big) J^{iso} w_{weight}. \quad (4.33)$$

Considering the third term, the stress can be split up according to 2.24. The deviatoric part is not dependent directly on the displacement

$$\frac{\partial {}^{n+1}\tau_{ij}}{\partial {}^{n+1}\hat{u}^\alpha} = \frac{\partial {}^{n+1}(\text{dev}(\tau_{ij}) + \frac{1}{3}\tau_{pp}\delta_{ij})}{\partial {}^{n+1}\hat{u}^\alpha} = \frac{\partial {}^{n+1}(pJ\delta_{ij})}{\partial {}^{n+1}\hat{u}^\alpha}. \quad (4.34)$$

Differentiating the hydrostatic part in 2.25, and the deformation gradient yields

$$\frac{\partial {}^{n+1}\tau_{ij}}{\partial {}^{n+1}\hat{u}^\alpha} = (\kappa {}^{n+1}J^2 + (\theta - \theta_0) \left(\frac{-3\beta\kappa}{2} \left[1 - \frac{1}{{}^{n+1}J^2} \right] \right)) {}^{n+1}C_{st}^{-1} B_{st}^\alpha ({}^{n+1}\hat{u}^\beta) \delta_{ij} \quad (4.35)$$

$$\frac{\partial {}^{n+1}F_{ij}^{-1}}{\partial {}^{n+1}\hat{u}^\alpha} = -{}^{n+1}F_{ik}^{-1n+1} F_{lj}^{-1} \frac{\partial N_k^\alpha}{\partial X_l}. \quad (4.36)$$

where δ_{ij} is the Kronecker's delta. For plastic response the derivative of the outer residual with respect to the internal variables are

$$\frac{\partial^{n+1}(F_{int})^\gamma}{\partial^{n+1}w} = \begin{cases} \frac{\partial^{n+1}(F_{int})^\gamma}{\partial^{n+1}\bar{b}_{ab}^e} = B_{ij}^\gamma ({}^{n+1}\hat{u}^\beta)^{n+1} F_{is}^{-1} \mu I_{stab}^{dev\ n+1} F_{jt}^{-1} J^{iso} w_{weight} \\ \frac{\partial^{n+1}(F_{int})^\gamma}{\partial^{n+1}\alpha} = 0^\gamma \\ \frac{\partial^{n+1}(F_{int})^\gamma}{\partial^{n+1}\theta} = B_{ij}^\gamma ({}^{n+1}\hat{u}^\beta)^{n+1} F_{is}^{-1} (-3\beta\kappa [{}^{n+1}J + \frac{1}{{}^{n+1}J}] \delta_{ij})^{n+1} F_{jt}^{-1} J^{iso} w_{weight} \end{cases} \quad (4.37)$$

For elastic response it reduces to

$$\frac{\partial^{n+1}(F_{int})^\gamma}{\partial^{n+1}w} = \begin{cases} \frac{\partial^{n+1}(F_{int})^\gamma}{\partial^{n+1}\bar{b}_{ab}^e} = B_{ij}^\gamma ({}^{n+1}\hat{u}^\beta)^{n+1} F_{is}^{-1} \mu I_{stab}^{dev\ n+1} F_{jt}^{-1} J^{iso} w_{weight} \\ \frac{\partial^{n+1}(F_{int})^\gamma}{\partial^{n+1}\theta} = B_{ij}^\gamma ({}^{n+1}\hat{u}^\beta)^{n+1} F_{is}^{-1} (-3\beta\kappa [J + \frac{1}{J}] \delta_{ij})^{n+1} F_{jt}^{-1} J^{iso} w_{weight} \end{cases} \quad (4.38)$$

where the deviatoric part of is I_{ijab}

$$I_{ijab} = \frac{1}{2}(\delta_{ia}\delta_{jb} + \delta_{ib}\delta_{ja}) \quad I_{ijab}^{dev} = I_{ijab} - \frac{1}{3}\delta_{ab}I_{ijab}. \quad (4.39)$$

The derivatives with respect to the previous time step n are also needed.

$$\frac{\partial^{n+1}(F_{int})^\gamma}{\partial^n \hat{u}^\alpha} = 0^{\gamma\alpha} \quad (4.40)$$

If n is a step with plastic response, the derivative of the outer residual with respect to the internal variables is

$$\frac{\partial^{n+1}(F_{int})^\gamma}{\partial^n w} = \begin{cases} \frac{\partial^{n+1}(F_{int})^\gamma}{\partial^n \bar{b}_{ab}^e} = 0^{\gamma\alpha} \\ \frac{\partial^{n+1}(F_{int})^\gamma}{\partial^n \alpha} = 0^\gamma \\ \frac{\partial^{n+1}(F_{int})^\gamma}{\partial^n \theta} = 0^\gamma \end{cases} \quad (4.41)$$

If n is a step with elastic response the derivative is

$$\frac{\partial^{n+1}(F_{int})^\gamma}{\partial^n w} = \begin{cases} \frac{\partial^{n+1}(F_{int})^\gamma}{\partial^n \bar{b}_{ab}^e} = 0^{\gamma\alpha} \end{cases} \quad (4.42)$$

Considering the mass matrix, differentiating this part with respect to the displacements results in

$$\frac{\partial^{n+1}}{\partial^{n+1}\hat{u}_\alpha} \left(c_1 \rho_0(\rho) N_{\delta\gamma} N_{\delta\beta}^{n+1} \hat{u}_\beta J^{iso} w_{weight} \right) = c_1 \rho_0(\rho) N_{\delta\gamma} N_{\delta\alpha} J^{iso} w_{weight}. \quad (4.43)$$

4.3.2 Derivatives of the local residual

Considering the local residual, if step $n + 1$ has elastic response there is no hardening i.e. ${}^{n+1}\alpha = {}^n\alpha$ and the yield function isn't necessary, nor possible to solve ($f \leq 0$ for elastic response). Considering the heat equation, another consequence of the elastic response is that there will be no evolution of the temperature, i.e. ${}^{n+1}\theta = {}^n\theta$ and the only equation needs solving for in the local residual is the flow rule C_1 as seen in 4.28. Therefore the derivative when $n + 1$ has elastic response reduces to

$$\frac{\partial^{n+1}C}{\partial^{n+1}w} = \left\{ \frac{\partial^{n+1}({}^1C_{ij})}{\partial^{n+1}\bar{b}_{ab}^e} = I_{ijab} \right. \quad (4.44)$$

When differentiating with respect to the previous time step n the derivatives differ depending on the combined response of time step n and $n + 1$. If $n + 1$ and n has elastic response the only state variable to differentiate with respect to is the left Cauchy-Green tensor which results in

$$\frac{\partial^{n+1}C}{\partial^n w} = \left\{ \frac{\partial^{n+1}({}^1C_{ij})}{\partial^n \bar{b}_{ab}^e} = {}^{n+1}\bar{f}_{ia} {}^{n+1}\bar{f}_{jb}. \right. \quad (4.45)$$

If the state n has deformed plastically, the local residual needs to be differentiated with respect to all the state variables as

$$\frac{\partial^{n+1}C}{\partial^n w} = \left\{ \begin{array}{l} \frac{\partial^{n+1}({}^1C_{ij})}{\partial^n \bar{b}_{ab}^e} = {}^{n+1}\bar{f}_{ia} {}^{n+1}\bar{f}_{jb} \\ \frac{\partial^{n+1}({}^1C_{ij})}{\partial^n \alpha} = 0_{ij} \\ \frac{\partial^{n+1}({}^1C_{ij})}{\partial^n \theta} = 0_{ij}. \end{array} \right. \quad (4.46)$$

If the step $n + 1$ is plastic, all the equations in the local residual needs to be considered as in 4.27. Differentiating this in the current time step then results in

$$\frac{\partial^{n+1}C}{\partial^{n+1}w} = \begin{cases} \frac{\partial^{n+1}(^1C_{ij})}{\partial^{n+1}\bar{b}_{ab}^e} = -\sqrt{\frac{2}{3}}\Delta\alpha \left(\delta_{ab}{}^{n+1}n_{ij} + {}^{n+1}\bar{b}_{tt}^e \frac{\partial^{n+1}n_{ij}}{\partial^{n+1}\bar{b}_{ab}^e} \right) - I_{ijab} \\ \frac{\partial^{n+1}(^1C_{ij})}{\partial^{n+1}\alpha} = -\sqrt{\frac{2}{3}}{}^{n+1}\bar{b}_{tt}^e{}^{n+1}n_{ij} \\ \frac{\partial^{n+1}(^1C_{ij})}{\partial^{n+1}\theta} = 0_{ij} \\ \frac{\partial^{n+1}(^2C)}{\partial^{n+1}\bar{b}_{ab}^e} = \mu^{n+1}n_{ab} \\ \frac{\partial^{n+1}(^2C)}{\partial^{n+1}\alpha} = -\sqrt{\frac{2}{3}} \left(\hat{h}(\theta)m\alpha^{m-1} + \hat{\sigma}_{y_\infty} \right) \\ \frac{\partial^{n+1}(^2C)}{\partial^{n+1}\theta} = \sqrt{\frac{2}{3}} \left(h\omega_h\alpha^m + \sigma_{y_\infty}\omega_h(1 - e^{-\delta\alpha}) + \sigma_{y_0}\omega_0 \right) \\ \frac{\partial^{n+1}(^3C)}{\partial^{n+1}\bar{b}_{ab}^e} = 0_{ab} \\ \frac{\partial^{n+1}(^3C)}{\partial^{n+1}\alpha} = \frac{\eta}{\rho_0 c}{}^{n+1}\hat{\sigma}_{y_0}(\theta) \\ \frac{\partial^{n+1}(^3C)}{\partial^{n+1}\theta} = -1 \end{cases} \quad (4.47)$$

where n_{ij} is the index notation of \mathbf{n} that is explained in 2.34 and the differentiation with respect to the left Cauchy-Green tensor is

$$\frac{\partial^{n+1}n_{ij}}{\partial^{n+1}\bar{b}_{ab}^e} = \sqrt{\frac{1}{{}^{n+1}d_{cd}^e{}^{n+1}d_{cd}^e}} \left(I_{ijab}^{dev} - {}^{n+1}n_{ab}^e{}^{n+1}n_{ij}^e \right) \quad (4.48)$$

Considering the differentiation with respect to previous time step, if n and $n + 1$ both are plastic the local residual is the plastic one described in 4.27 and the derivation has

to be done for all the state variables as

$$\frac{\partial^{n+1}C}{\partial^n w} = \begin{cases} \frac{\partial^{n+1}(^1C_{ij})}{\partial^n \bar{b}_{ab}^e} = {}^{n+1}\bar{f}_{ia} {}^{n+1}\bar{f}_{jb} \\ \frac{\partial^{n+1}(^1C_{ij})}{\partial^n \alpha} = \sqrt{\frac{2}{3}} {}^{n+1}\bar{b}_{tt}^e {}^{n+1}n_{ij}^e \\ \frac{\partial^{n+1}(^1C_{ij})}{\partial^n \theta} = 0_{ij} \\ \frac{\partial^{n+1}(^2C)}{\partial^n \bar{b}_{ab}^e} = 0_{ab} \\ \frac{\partial^{n+1}(^2C)}{\partial^n \alpha} = 0 \\ \frac{\partial^{n+1}(^2C)}{\partial^n \theta} = 0 \\ \frac{\partial^{n+1}(^3C)}{\partial^n \bar{b}_{ab}^e} = 0_{ab} \\ \frac{\partial^{n+1}(^3C)}{\partial^n \alpha} = -\frac{\eta}{\rho_0^C} \hat{\sigma}^{(n+1)\theta} \\ \frac{\partial^{n+1}(^3C)}{\partial^n \theta} = 1. \end{cases} \quad (4.49)$$

Continuing in similar fashion, if step n is elastic the full local residual needs to be differentiated with respect to the left Cauchy-Green tensor as

$$\frac{\partial^{n+1}C}{\partial^n w} = \begin{cases} \frac{\partial^{n+1}(^1C_{ij})}{\partial^n \bar{b}_{ab}^e} = {}^{n+1}\bar{f}_{ia} {}^{n+1}\bar{f}_{jb} \\ \frac{\partial^{n+1}(^2C_{ij})}{\partial^n \bar{b}_{ab}^e} = 0_{ab} \\ \frac{\partial^{n+1}(^3C_{ij})}{\partial^n \bar{b}_{ab}^e} = 0_{ab}. \end{cases} \quad (4.50)$$

The derivatives of the local residual with respect to the displacement are also necessary for finding the gradient and for plastic response in time step $n + 1$ the derivative is

$$\frac{\partial^{n+1}C}{\partial^{n+1}\hat{u}^\alpha} = \begin{cases} \frac{\partial^{n+1}(^1C_{ij})}{\partial^{n+1}\hat{u}^\alpha} = \frac{\partial^{n+1}\bar{f}_{ik} {}^{n+1}\bar{b}_{kl}^e \bar{f}_{jl}}{\partial^{n+1}\hat{u}^\alpha} + {}^{n+1}\bar{f}_{ik} {}^{n+1}\bar{b}_{kl}^e \frac{\partial^{n+1}\bar{f}_{jl}}{\partial^{n+1}\hat{u}^\alpha} \\ \frac{\partial^{n+1}(^2C)}{\partial^{n+1}\hat{u}^\alpha} = 0^\alpha \\ \frac{\partial^{n+1}(^3C)}{\partial^{n+1}\hat{u}^\alpha} = 0^\alpha \end{cases} \quad (4.51)$$

and if no plastic deformation has occurred in $n + 1$ the result is

$$\frac{\partial^{n+1}C}{\partial^{n+1}\hat{u}^\alpha} = \left\{ \frac{\partial^{n+1}(^1C_{ij})}{\partial^{n+1}\hat{u}^\alpha} = \frac{\partial^{n+1}\bar{f}_{ik}}{\partial^{n+1}\hat{u}^\alpha} {}^n\bar{b}_{kl}^e \bar{f}_{jl} + {}^{n+1}\bar{f}_{ik} {}^n\bar{b}_{kl}^e \frac{\partial^{n+1}\bar{f}_{jl}}{\partial^{n+1}\hat{u}^\alpha} \right. \quad (4.52)$$

where the differentiation of the relative deformation gradient is

$$\frac{\partial^{n+1}\bar{f}_{ij}}{\partial^{n+1}\hat{u}^\alpha} = \left(\frac{{}^n J}{{}^{n+1} J} \right)^{1/3} \frac{\partial N_i^\alpha}{\partial X_k} {}^n F_{kj}^{-1} - \frac{1}{3} {}^{n+1}\bar{f}_{ij} {}^{n+1}C_{st}^{-1} B_{st}^\alpha ({}^{n+1}u^\beta). \quad (4.53)$$

Considering differentiation with respect to the displacement for the previous time steps the derivative is

$$\frac{\partial^{n+1}C}{\partial^n \hat{u}^\alpha} = \begin{cases} \frac{\partial^{n+1}(^1C_{ij})}{\partial^n \hat{u}^\alpha} = \frac{\partial^{n+1}\bar{f}_{ik}}{\partial^n \hat{u}^\alpha} {}^n\bar{b}_{kl}^e \bar{f}_{jl} + {}^{n+1}\bar{f}_{ik} {}^n\bar{b}_{kl}^e \frac{\partial^{n+1}\bar{f}_{jl}}{\partial^n \hat{u}^\alpha} \\ \frac{\partial^{n+1}(^2C)}{\partial^n \hat{u}^\alpha} = 0^\alpha \\ \frac{\partial^{n+1}(^3C)}{\partial^n \hat{u}^\alpha} = 0^\alpha. \end{cases} \quad (4.54)$$

if the response is plastic. If the response in $n + 1$ is elastic the derivative is

$$\frac{\partial^{n+1}C}{\partial^n \hat{u}^\alpha} = \left\{ \frac{\partial^{n+1}(^1C_{ij})}{\partial^n \hat{u}^\alpha} = \frac{\partial^{n+1}\bar{f}_{ik}}{\partial^n \hat{u}^\alpha} {}^n\bar{b}_{kl}^e \bar{f}_{jl} + {}^{n+1}\bar{f}_{ik} {}^n\bar{b}_{kl}^e \frac{\partial^{n+1}\bar{f}_{jl}}{\partial^n \hat{u}^\alpha} \right. \quad (4.55)$$

where the derivative of the relative deformation gradient is

$$\frac{\partial^{n+1}\bar{f}_{ij}}{\partial^n \hat{u}^\alpha} = \frac{1}{3} {}^{n+1}\hat{f}_{ij} {}^n C_{st}^{-1} B_{st}^\alpha ({}^n \hat{u}^\beta) - {}^{n+1}\bar{f}_{is} {}^n F_{lj}^{-1} \frac{\partial N_s^\alpha}{\partial X_l}. \quad (4.56)$$

4.3.3 Implicit derivatives of the objective function

The total plastic work defined in 4.1 is a summation of the plastic work in each time step

$$W_p = \dots + \left(K'({}^{n+1}\alpha, {}^{n+1}\theta) + \hat{\sigma}_{y_0}({}^{n+1}\theta) \right) ({}^{n+1}\alpha - {}^n\alpha) J^{iso} w_{weight} \\ + \left(K'({}^{n+2}\alpha, {}^{n+2}\theta) + \hat{\sigma}_{y_0}({}^{n+2}\theta) \right) ({}^{n+2}\alpha - {}^{n+1}\alpha) J^{iso} w_{weight} + \dots \quad (4.57)$$

where

$$K'({}^{n+1}\alpha, {}^{n+1}\theta) = h[1 - \omega_h({}^{n+1}\theta - \theta_0)]^{n+1} \alpha^m + \sigma_{y_\infty} [1 - \omega_h({}^{n+1}\theta - \theta_0)] (1 - e^{-\delta^{n+1}\alpha}) \quad (4.58)$$

cf. in 2.32. Note that the objective function does not depend on the displacement, therefore only the derivatives with respect to the internal variables and the density are required. In the following section only the non-zero derivatives are presented Starting with the internal variables, differentiating the objective function with respect to $\bar{\mathbf{b}}^e$ results in

$$\left\{ \begin{array}{l} \frac{\partial G}{\partial^{n+1}\bar{b}_{ij}^e} = 0_{ij} \\ \frac{\partial G}{\partial^{n+1}\alpha} = \left\{ \frac{\partial K'({}^{n+1}\alpha, {}^{n+1}\theta)}{\partial^{n+1}\alpha} ({}^{n+1}\alpha - {}^n\alpha) + K'({}^{n+1}\alpha, {}^{n+1}\theta) \right. \\ \qquad \qquad \qquad \left. - \left(K'({}^{n+2}\alpha, {}^{n+2}\theta) + \hat{\sigma}_{y_0}({}^{n+2}\theta) \right) \right\} J^{iso}w_{weight} \\ \frac{\partial G}{\partial^{n+1}\theta} = - \left(h\omega_h {}^{n+1}\alpha^m + \sigma_{y_\infty}\omega_h(1 - e^{-\delta^{n+1}\alpha}) + \sigma_{y_0}\omega_0 \right) ({}^{n+1}\alpha - {}^n\alpha) J^{iso}w_{weight} \end{array} \right. \quad (4.59)$$

if both step $n + 1$ and $n + 2$ have plastic response where

$$\frac{\partial K'({}^{n+1}\alpha, {}^{n+1}\theta)}{\partial^{n+1}\alpha} = \hat{h}({}^{n+1}\theta)m^{n+1}\alpha^m + \hat{\sigma}_{y_\infty}({}^{n+1}\theta) \cdot (1 + \delta e^{-\delta^{n+1}\alpha}). \quad (4.60)$$

$$(4.61)$$

$$\left\{ \begin{array}{l} \frac{\partial G}{\partial^{n+1}\bar{b}_{ij}^e} = 0_{ij} \\ \frac{\partial G}{\partial^{n+1}\alpha} = \left\{ \frac{\partial K'({}^{n+1}\alpha, {}^{n+1}\theta)}{\partial^{n+1}\alpha} ({}^{n+1}\alpha - {}^n\alpha) + K'({}^{n+1}\alpha, {}^{n+1}\theta) \right\} J^{iso}w_{weight} \\ \frac{\partial G}{\partial^{n+1}\theta} = - \left(h\omega_h {}^{n+1}\alpha^m + \sigma_{y_\infty}\omega_h(1 - e^{-\delta^{n+1}\alpha}) + \sigma_{y_0}\omega_0 \right) ({}^{n+1}\alpha - {}^n\alpha) J^{iso}w_{weight} \end{array} \right. \quad (4.62)$$

Note that in the last step-term in 4.57, $n + 1 = M$, $n+2$ doesn't exist.

4.3.4 The explicit term

The explicit term, cf. 4.14, requires the derivatives with respect to the design variable ϕ_e . The RAMP interpolation introduced in section 4.1 makes the material properties κ, μ dependent on the density. From the same section it was concluded that the filtered and thresholded density could be expressed as $c = H(\tilde{c}(\phi))$. When differentiating with

respect to the design variable this must be taken into account

$$\frac{\partial(F_{int})_{ij}^\gamma}{\partial\phi} = \frac{\partial(F_{int})_{ij}^\gamma}{\partial\rho} \frac{\partial\rho}{\partial\tilde{\rho}} \frac{\partial\tilde{\rho}}{\partial\phi} = \left(\frac{\partial\mu}{\partial\rho} d_{ij}^e - \frac{\partial\kappa}{\partial\rho} \left[[J^2 - 1] - (\theta - \theta_0)(3\beta[J + \frac{1}{J}]) \right] \delta_{ij} \right) \frac{\partial\rho}{\partial\tilde{\rho}} \frac{\partial\tilde{\rho}}{\partial\phi} \quad (4.63)$$

where $\partial\mu/\partial\rho$ and $\partial\kappa/\partial\rho$ comes from differentiation of 4.5

$$\begin{aligned} \frac{\partial\mu}{\partial\rho} &= \frac{1+q}{(1+q(1-\rho))^2} (\mu_1 - \mu_0) \\ \frac{\partial\kappa}{\partial\rho} &= \frac{1+q}{(1+q(1-\rho))^2} (\kappa_1 - \kappa_0). \end{aligned}$$

For the local residual the derivatives are

$$\frac{\partial^{n+1}({}^1C_{ij})}{\partial\phi} = 0_{ij} \quad (4.64)$$

$$\begin{aligned} \frac{\partial^{n+1}({}^2C)}{\partial\phi} &= \left[\frac{\partial\mu}{\partial\rho} \sqrt{\bar{d}_{ij}^e \bar{d}_{ij}^e} \right. \\ &\quad \left. - \sqrt{\frac{2}{3}} \left(\frac{\partial h}{\partial\rho} [1 - \omega_h^{(n+1)\theta - \theta_0}]^{n+1} \alpha^m + \frac{\partial\sigma_{y_\infty}}{\partial\rho} [1 - \omega_h^{(n+1)\theta - \theta_0}] (1 - e^{-\delta^{n+1}\alpha}) \right. \right. \\ &\quad \left. \left. + \frac{\partial\sigma_{y_0}}{\partial\rho} [1 - \omega_0^{(n+1)\theta - \theta_0}] \right) \right] \frac{\partial\rho}{\partial\tilde{\rho}} \frac{\partial\tilde{\rho}}{\partial\phi} \quad (4.65) \end{aligned}$$

$$\frac{\partial^{n+1}({}^3C)}{\partial\phi} = \left(\frac{\eta}{\rho_0 c} \frac{\partial\sigma_{y_0}}{\partial\rho} [1 - \omega_0^{(n+1)\theta - \theta_0}] \right) \frac{\partial\rho}{\partial\tilde{\rho}} \frac{\partial\tilde{\rho}}{\partial\phi} \quad (4.66)$$

where

$$\begin{aligned} \frac{\partial\sigma_{y_0}}{\partial\rho} &= \frac{1+q}{(1+q(1-\rho))^2} ((\sigma_{y_0})_1 - (\sigma_{y_0})_0) \\ \frac{\partial\sigma_{y_\infty}}{\partial\rho} &= \frac{1+q}{(1+q(1-\rho))^2} ((\sigma_{y_\infty})_1 - (\sigma_{y_\infty})_0) \\ \frac{\partial h}{\partial\rho} &= \frac{1+q}{(1+q(1-\rho))^2} (h_1 - h_0) \end{aligned}$$

Considering the mass matrix, differentiating this with respect to the design variable results in

$$\frac{\partial^{n+1}}{\partial\phi} \left(c_1 \rho_0(\rho) N_{\delta\gamma} N_{\delta\beta}^{n+1} \hat{u}_\beta J^{iso} w_{weight} \right) = c_1 N_{\delta\gamma} N_{\delta\beta}^{n+1} \hat{u}_\beta J^{iso} w_{weight} \frac{\partial\rho_0(\rho)}{\partial\rho} \frac{\partial\rho}{\partial\tilde{\rho}} \frac{\partial\tilde{\rho}}{\partial\phi} \quad (4.67)$$

where

$$\frac{\partial\rho_0(\rho)}{\partial\rho} = \frac{1+q}{(1+q(1-\rho))^2} ((\rho_0)_1 - (\rho_0)_0). \quad (4.68)$$

4.4 Remarks about sensitivities

The sensitivities corresponding to the thermomechanical model are derived in the previous section. Because of time-limitation, these sensitivities are not implemented in the FE-program, instead to save time, the sensitivities from the quasi static elasto-plastic model used in [19] are used. The objective function and the solution to the equilibrium problem corresponds to the thermomechanical problem though. These, approximated sensitivities, are then compare to a numerical sensitivities using numeric differentiation, explained in section 4.3. A ratio between the numerical differentiated objective function $\partial W_p(\boldsymbol{\phi})/\partial \phi_j$ and the analytically calculated approximation was used for comparison. The thermomechanical model is also compared to the unmodified model in elasto-plastic model [19].

Chapter 5

Results

The model is tested on a structure as presented in figure 5.1. On the right and left side, the structure has fixed prescribed displacement, and a prescribed displacement in a cone shape is applied in the middle. The structure measures 20mm in width and 5mm in height. The material parameters are chosen as to match those of steel as in table 5.1. The reference temperature is chosen as room temperature and the parameters that

κ	μ	σ_{y0}	h	$\sigma_{\infty 0}$	δ	ρ	θ_0	ω_0	ω_h	β
164	80	400	18	715	16.9	7800	293	$2 \cdot 10^{-3}$	$1 \cdot 10^{-3}$	$1.5 \cdot 10^5$
GPa	GPa	MPa	MPa	MPa		kg/m ³	K	K ⁻¹	K ⁻¹	

Table 5.1 Material properties for steel

determine the temperature influence is also data for steel, and can be found in e.g. [17]. They are chosen as a linear approximation in the temperature region 273 - 373 K. The thermal expansion coefficient β was chosen according to [3]. This, together with the specific heat c are assumed to be temperature independent for the temperature range considered. The RAMP penalization parameters were chosen as $q = 6$ for $\kappa, \mu, h, \sigma_{y0}$ and ρ . For the initial flow stress, a slightly lower penalization at $q = 4$ were chosen

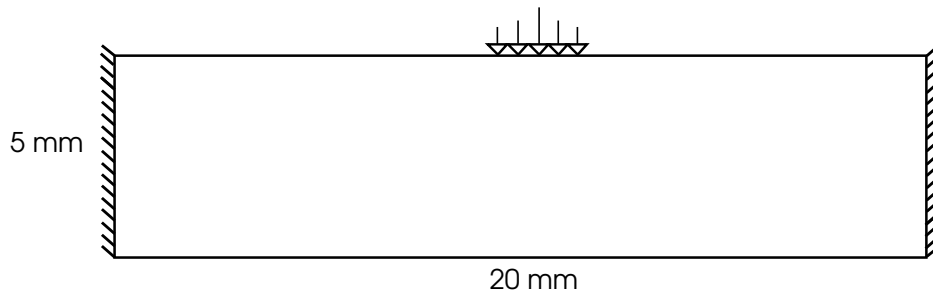


Fig. 5.1 Double clamped beam used to illustrate the model.

according to [19]. The Newmark stability parameters were kept constant at $\gamma = 0.5$ and $\beta = 0.25$ for stability.

A comparison of the sensitivity from the isothermal problem presented in [19] versus the numerical differentiated sensitivity is seen in table 5.2. The comparison is made as a ratio between the differentiated objective function with respect to the design variable $\partial W_p / \partial \phi_e$ for the two computed sensitivities.

Displacement	0.008	0.3	0.8	2.5
Error percentage	0.0024 %	0.041%	0.3142%	14.86 %

Table 5.2 Comparison of the thermomechanical model using the sensitivities in [19] versus the numerically differentiated sensitivities for some prescribed displacement

For the case with the thermomechanical model using the sensitivities of [19], the deformation for 0.8mm prescribed displacement can be seen in figure 5.2. Here the use of symmetry can be seen, and the right part of the structure is presented. The accumulated temperature is shown in figure 5.3 together with a plot of the plastic work in each element, figure 5.4. The total plastic work versus the MMA-iterations can be seen in figure 5.5.

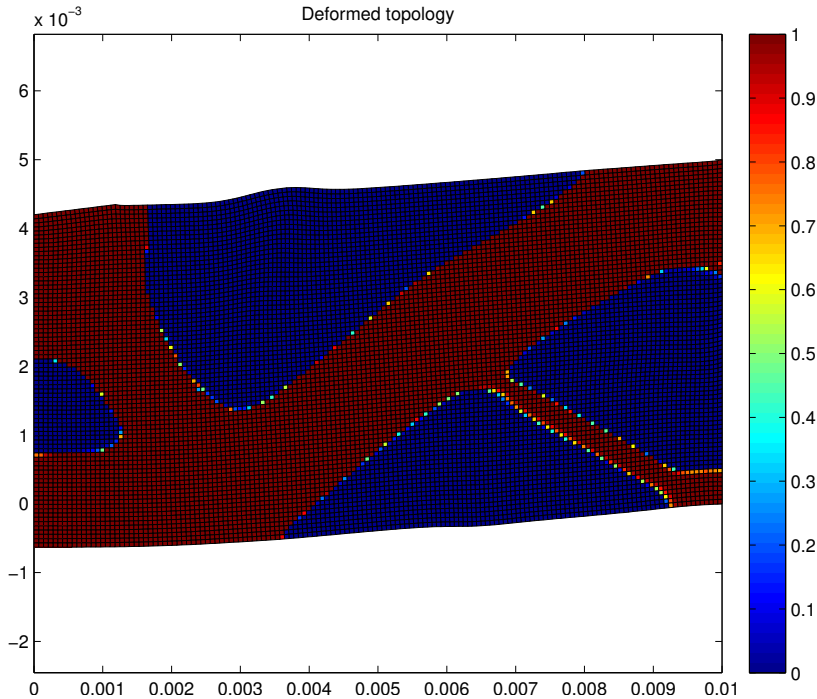


Fig. 5.2 Deformed topology for thermomechanical model with 0.8mm prescribed displacement in middle of structure

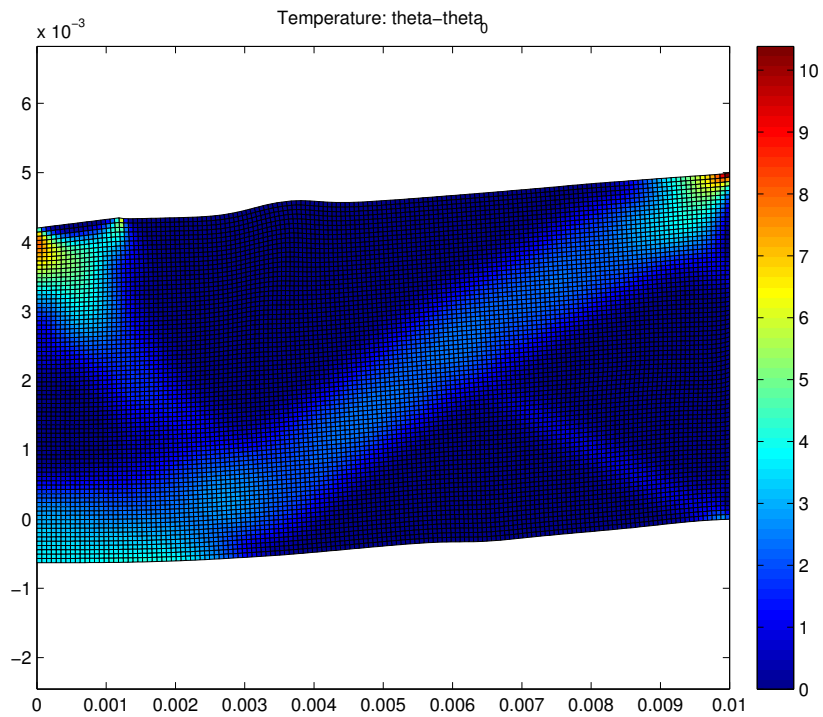


Fig. 5.3 Generated temperature in the structure using the thermomechanical model with 0.8mm prescribed displacement

Considering larger displacements, the structure was also subjected to a prescribed displacements of 2.5mm as shown in figure 5.6. For comparison, the isothermal version presented in [19] was also computed, see figure 5.7.

The temperature for prescribed displacement can be seen in 5.8 together with the plastic work for each element (figure 5.9) and the progress of the total plastic work as function of MMA - iterations (figure 5.10). A temperature increase of 30°C represents a lowered yield stress by 6% ie. from 400MPa to 376MPa.

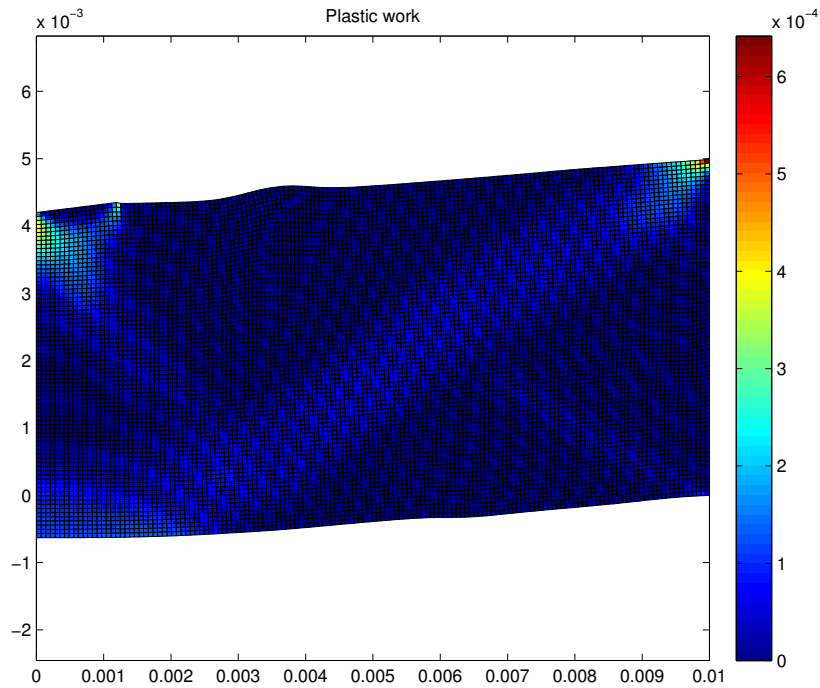


Fig. 5.4 Generated plastic work in the structure using the thermomechanical model with 0.8mm prescribed displacement

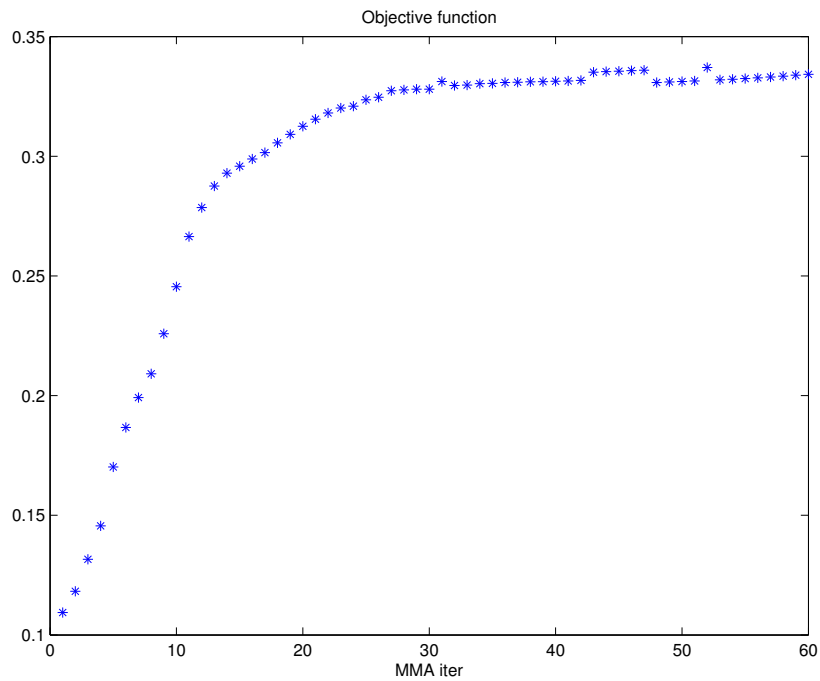


Fig. 5.5 Generated plastic work in the structure using the thermomechanical model with 0.8mm prescribed displacement

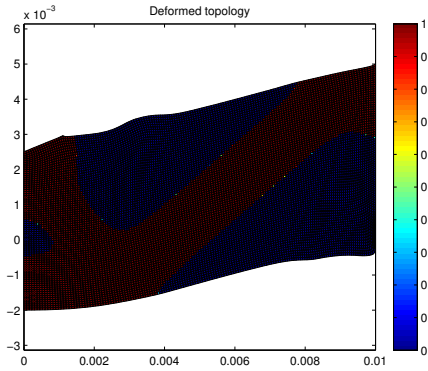


Fig. 5.6 Deformed topology for thermomechanical model with 2.5mm prescribed disp.

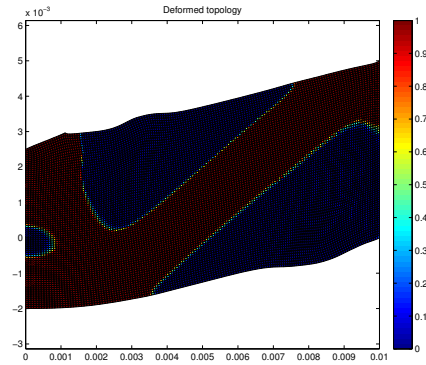


Fig. 5.7 Deformed topology, isothermal model with 2.5mm prescribed disp.

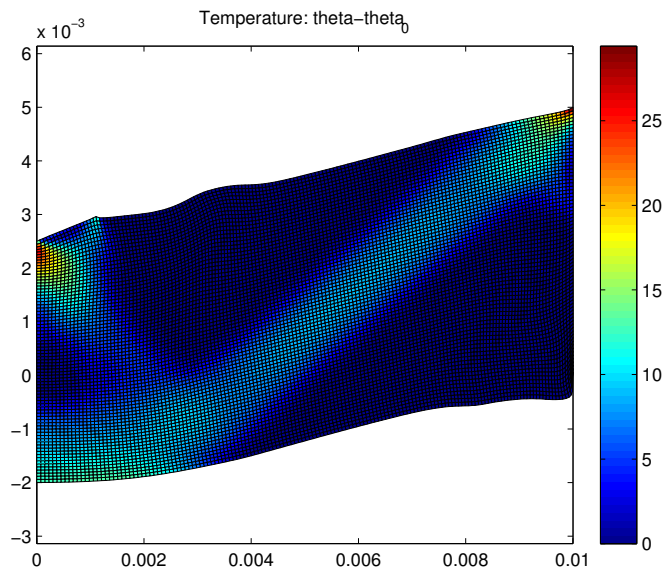


Fig. 5.8 Generated temperature in the structure using the thermomechanical model with 2.5mm prescribed displacement

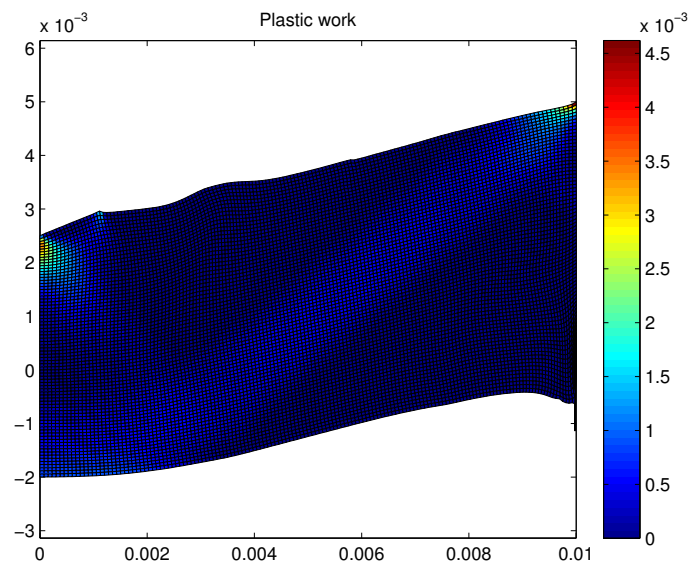


Fig. 5.9 Generated plastic work in the structure using the thermomechanical model with 2.5mm prescribed displacement

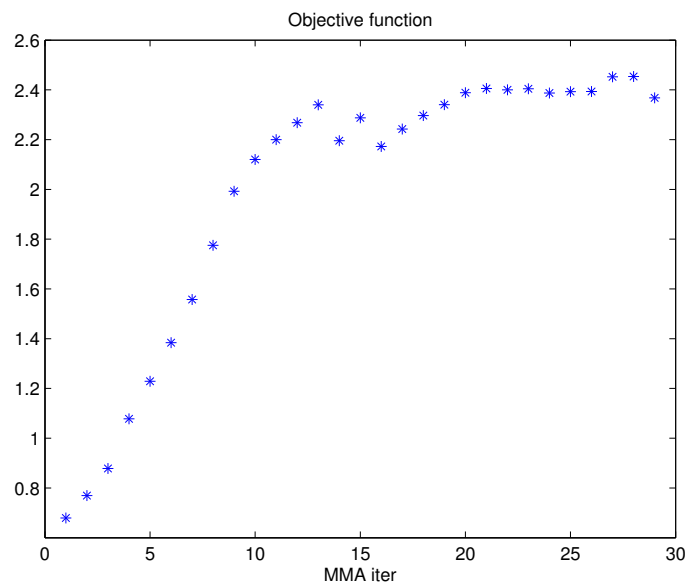


Fig. 5.10 Total generated plastic work in the structure using the thermomechanical model with 2.5mm prescribed displacement

Chapter 6

Discussion

Comparing the sensitivities in 5.2 it can be seen that for small displacements for the double clamped beam, the isothermal sensitivity from [19] can be used, however, it can be clearly seen that if greater displacement are to be used such that large amount of plastic work is produced, the thermomechanical model needs to be implemented into the sensitivities. This can be done using the adjoint method derived in [19] with the modification as suggested in section 4.3.

The temperature distribution in figure 5.8 is focused around fixed boundary conditions at the sides of the structure and where the prescribed displacements in the middle is located. In these area the properties of the material will change and eg. thermal softening can be observed.

In the project, the simplest temperature dependency have been implemented for the material parameters like the initial yield stress σ_{y0} , the saturation stress $\sigma_{\infty 0}$ and the hardening modulus h . The linear approximation could easily be replaced by a more realistic, complex approximation. For the constant specific heat c , this could also be temperature dependent. For austentic stainless steel c is almost linear as shown in [17], so perhaps a linear approximation would be ideal. This could be done with some slightly modification of the free energy function as c is defined by this as $c = -\theta \partial_{\theta\theta}^2 \Psi$.

The approximation that heat conduction does not take place due to rapid deformation needs to be investigated as well. How fast must the deformation occur in order for this to still make a good approximation and how does viscous effects effect the result?

References

- [1] Christensen, P. W. and Klarbring, A. (2008). *An introduction to structural optimization*, volume 153. Springer Science & Business Media.
- [2] Guest, J. K., Prévost, J. H., and Belytschko, T. (2004). Achieving minimum length scale in topology optimization using nodal design variables and projection functions. *International journal for numerical methods in engineering*, 61(2):238–254.
- [3] Håkansson, P., Wallin, M., and Ristinmaa, M. (2005). Comparison of isotropic hardening and kinematic hardening in thermoplasticity. *International Journal of Plasticity*, 21(7):1435–1460.
- [4] Heinbockel, J. H. (2001). *Introduction to tensor calculus and continuum mechanics*, volume 52. Trafford.
- [5] Hill, R. (1998). *The Mathematical Theory of Plasticity*. Oxford Classic Texts in the Ph. Clarendon Press.
- [6] Jönsson, V. and Wingren, E. (2015). Topology optimization for elasto-plasticity. *TFHF-5203*.
- [7] Krenk, S. (2009). *Non-linear modeling and analysis of solids and structures*. Cambridge University Press.
- [8] Kröner, E. (1960). General continuum theory of dislocations and self-stresses. *Arch. Rat. Mech. Anal*, 4:18–334.
- [9] Laurenceau, J. and Meaux, M. (2008). Comparison of gradient and response surface based optimization frameworks using adjoint method. In *49th AIAA/ASME/ASCE/AHS/ASC Structures, Structural Dynamics, and Materials Conference, 16th AIAA/ASME/AHS Adaptive Structures Conference, 10th AIAA Non-Deterministic Approaches Conference, 9th AIAA Gossamer Spacecraft Forum, 4th AIAA Multidisciplinary Design Optimization Specialists Conference*, page 1889.
- [10] Lazarov, B. S. and Sigmund, O. (2011). Filters in topology optimization based on helmholtz-type differential equations. *International Journal for Numerical Methods in Engineering*, 86(6):765–781.
- [11] Michaleris, P., Tortorelli, D. A., and Vidal, C. A. (1994). Tangent operators and design sensitivity formulations for transient non-linear coupled problems with applications to elastoplasticity. *International Journal for Numerical Methods in Engineering*, 37(14):2471–2499.

-
- [12] Mroz, Z. and Oliferuk, W. (2002). Energy balance and identification of hardening moduli in plastic deformation processes. *International Journal of Plasticity*, 18(3):379–397.
- [13] Ottosen, N. S. and Petersson, H. (1992). *Introduction to the finite element method*. Prentice-Hall.
- [14] Simo, J. and Miehe, C. (1992). Associative coupled thermoplasticity at finite strains: Formulation, numerical analysis and implementation. *Computer Methods in Applied Mechanics and Engineering*, 98(1):41–104.
- [15] Stolpe, M. and Svanberg, K. (2001). An alternative interpolation scheme for minimum compliance topology optimization. *Structural and Multidisciplinary Optimization*, 22(2):116–124.
- [16] Svanberg, K. (1987). The method of moving asymptotes—a new method for structural optimization. *International journal for numerical methods in engineering*, 24(2):359–373.
- [17] Tavassoli, A. (1995). Assessment of austenitic stainless steels. *Fusion Engineering and Design*, 29:371–390.
- [18] Taylor, G. I. and Quinney, H. (1934). The latent energy remaining in a metal after cold working. *Proceedings of the Royal Society of London. Series A, Containing Papers of a Mathematical and Physical Character*, 143(849):307–326.
- [19] Wallin, M., Jönsson, V., and Wingren, E. (2016). Topology optimization based on finite strain plasticity. *Structural and multidisciplinary optimization*, 54(4):783–793.
- [20] Zdebel, U. and Lehmann, T. (1987). Some theoretical considerations and experimental investigations on a constitutive law in thermoplasticity. *International journal of plasticity*, 3(4):369–389.

Appendix A

Local solution

A.1

The integrated heat equation with approximation for mechanical work in section 3.3

$$\begin{aligned} {}^{n+1}\theta - {}^n\theta &= \frac{\eta}{\rho_0 c} \hat{y}_0 ({}^{n+1}\alpha - {}^n\alpha) = \frac{\eta}{\rho_0 c} y_0(\theta_0) [1 - \omega_0 ({}^{n+1}\theta - \theta_0)] ({}^{n+1}\alpha - {}^n\alpha) = \\ &\quad \frac{\eta}{\rho_0 c} y_0(\theta_0) [1 + \omega_0 \theta_0] ({}^{n+1}\alpha - {}^n\alpha) - \frac{\eta}{\rho_0 c} y_0(\theta_0) \omega_0 {}^{n+1}\theta ({}^{n+1}\alpha - {}^n\alpha) \end{aligned}$$

yields an explicit expression for $\theta(\alpha)$

$${}^{n+1}\theta({}^n\alpha, {}^{n+1}\alpha) = \frac{{}^n\theta + \frac{\eta}{\rho_0 c} y_0(\theta_0) [1 + \omega_0 \theta_0] ({}^{n+1}\alpha - {}^n\alpha)}{1 + \frac{\eta}{\rho_0 c} y_0(\theta_0) \omega_0 ({}^{n+1}\alpha - {}^n\alpha)} \quad (\text{A.1})$$

Taylor expansion of yield function around state ${}^{n+1}$ updates the state

$$f = f + \frac{\partial f}{\partial \alpha} d\alpha \quad (\text{A.2})$$

where $d\alpha$ is solved for. The derivative of A.1

$$\begin{aligned} \frac{\partial {}^{n+1}\theta}{\partial {}^{n+1}\alpha} &= \frac{\frac{\eta}{\rho_0 c} y_0(\theta_0) [1 + \omega_0 \theta_0]}{1 + \frac{\eta}{\rho_0 c} y_0(\theta_0) \omega_0 ({}^{n+1}\alpha - {}^n\alpha)} - \\ &\quad - \frac{{}^n\theta + \frac{\eta}{\rho_0 c} y_0(\theta_0) [1 + \omega_0 \theta_0] ({}^{n+1}\alpha - {}^n\alpha)^2}{1 + \frac{\eta}{\rho_0 c} y_0(\theta_0) \omega_0 ({}^{n+1}\alpha - {}^n\alpha)} \cdot \frac{\eta}{\rho_0 c} y_0(\theta_0) \omega_0 \end{aligned}$$

$$\begin{aligned} \frac{\partial^{n+1} K'}{\partial^{n+1} \alpha} &= h(\theta_0)[1 - \omega_h({}^{n+1}\theta - \theta_0)] - h(\theta_0)\omega_h \frac{\partial^{n+1}\theta}{\partial^{n+1}\alpha} + \\ &\quad + y_{0,\infty}(\theta_0)[1 - \omega_h({}^{n+1}\theta - \theta_0)]\delta^{-\delta^{n+1}\alpha} - y_{0,\infty}(\theta_0)\omega_h \frac{\partial^{n+1}\theta}{\partial^{n+1}\alpha} (1 - e^{-\delta^{n+1}\alpha}) \\ \frac{\partial^{n+1} \hat{y}_0}{\partial^{n+1} \alpha} &= -y_0(\theta_0)\omega_0 \frac{\partial^{n+1}\theta}{\partial^{n+1}\alpha} \end{aligned}$$

Appendix B

Derivation of the algorithmic stiffness tensor

In order to preserve the second order convergence rate of the Newton-Raphson algorithm the continuum tangent stiffness needs to be replaced by the algorithmic tangent stiffness (3.17) that relates the stresses to the strains in the discretized system. Beginning by integrating the stress-strain relation

$$S_{AB} = \frac{\partial S_{AB}}{\partial E_{kl}} dE_{kl} \quad (\text{B.1})$$

using the backward Euler method results in

$${}^{(2)}S_{AB} = {}^{(1)}S_{AB} + \left. \frac{\partial S_{AB}}{\partial E_{kl}} \right|_{(2)} dE_{kl} \quad (\text{B.2})$$

where the derivative is rewritten with the Kirchhoff stress as

$$\left. \frac{\partial S_{AB}}{\partial E_{kl}} \right|_{(2)} = \frac{\partial(F_{Ai}^{-1} \tau_{ij} F_{Bj}^{-1})}{\partial C_{st}} \frac{\partial C_{st}}{\partial E_{kl}} = \frac{\partial(F_{Ai}^{-1} F_{Bj}^{-1} (\text{dev}(\tau_{ij}) + \frac{1}{3} \text{tr}(\tau) \delta_{ij}))}{\partial C_{st}} \frac{\partial C_{st}}{\partial E_{kl}}. \quad (\text{B.3})$$

From 3.28 the deviatoric part can be split up in a trial stress and back stress. The result is a stress in three terms like

$$\left. \frac{\partial S_{AB}}{\partial E_{kl}} \right|_{(2)} = \frac{\overset{\textcircled{1}}{\partial(F_{Ai}^{-1} F_{Bj}^{-1} (\text{dev}(\tau_{ij}^{trial}) - 2\bar{\mu} \Delta \lambda n_{ij} + \frac{1}{3} \text{tr}(\tau) \delta_{ij}))}}{\partial C_{st}} \frac{\partial C_{st}}{\partial E_{kl}} \quad (\text{B.4})$$

The first terms is differentiated as ①:

$$\begin{aligned} \frac{\partial}{\partial C_{st}} \left(-2/3 J \left[{}^n G_{AB}^p - \frac{1}{3} C_{xy}^n G_{xy}^p C_{AB}^{-1} \right] \right) &= \dots \\ &= F_{si}^{-1} F_{tj}^{-1} \left[\|\text{dev}(\tau^{trial})\| \left(n_{ai} n_{aj} - \frac{1}{3} \delta_{ij} \right) + \frac{\mu \text{tr}(\bar{b}^{e,trial})}{3} n_{ij} \right] \end{aligned}$$

The derivative of the second term is ②:

$$\begin{aligned} \frac{\partial S_{ab}}{\partial C_{st}} &= \frac{\partial}{\partial C_{st}} \left(\frac{\bar{\mu} \Delta \lambda \mu}{\|\text{dev} \tau^{trial}\|} \left[J^{2/3} (G_{ab}^{p,n} - \frac{1}{3} C_{xy} G_{xy}^{p,n} C_{ab}^{-1}) \right] \right) = \\ &= -F_{ai}^{-1} F_{bj}^{-1} F_{sx}^{-1} F_{ty}^{-1} \left[\bar{\mu} \beta_3 n_{ij} n_{xy} + \bar{\mu} \beta_4 n_{ij} \text{dev}(n_{ax} n_{ay}) - \right. \\ &\quad \left. - \beta_1 \left(\bar{\mu} [I_{ijxy} - \frac{1}{3} \delta_{ij} \delta_{xy}] - \frac{\|\text{dev}(\tau^{trial})\|}{3} [n_{ij} \delta_{xy} + \delta_{ij} n_{xy}] \right) \right] \end{aligned}$$

with

$$\begin{aligned} \beta_1 &= \frac{2\bar{\mu} \Delta \lambda}{\|\text{dev}(\tau^{trial})\|} \\ \beta_2 &= \frac{2}{3} \frac{\|\text{dev}(\tau^{trial})\|}{\bar{\mu}} \Delta \lambda \left(1 - \frac{1}{\beta_0} \right) \\ \beta_3 &= \beta_2 + \frac{1}{\beta_0} - \beta_1 \\ \beta_4 &= \frac{\|\text{dev}(\tau^{trial})\|}{\bar{\mu}} \left(\frac{1}{\beta_0} - \beta_1 \right) \end{aligned}$$

and the third term is ③

$$\begin{aligned} \frac{\partial}{\partial C_{st}} \left(C_{AB} \frac{1}{3} \text{tr}(\tau^{trial}) \right) &= \dots \\ &F_{Ap}^{-1} F_{Si}^{-1} F_{tu}^{-1} F_{Bv}^{-1} \left[\frac{1}{3} \text{tr}(\tau^{trial}) \frac{1}{2} (\delta_{pi} \delta_{uv} + \delta_{ui} \delta_{pv}) + \left(\kappa J^2 + (\theta - \theta_0) (-3\beta\kappa \left[\frac{J}{2} - \frac{1}{2J} \right]) \right) \delta_{ui} \delta_{pv} \right. \\ &\quad \left. + \frac{\partial \theta}{\partial \alpha} \frac{\partial \alpha}{\partial \Delta \lambda} \frac{1}{2\beta_0} \left(\left[1 - \frac{2\|\text{dev}(\tau^{trial})\|}{3\bar{\mu}} \Delta \lambda \right] n_{iu} \delta_{pv} + \frac{\|\text{dev}(\tau^{trial})\|}{\bar{\mu}} \text{dev}(n_{ai} n_{au}) \delta_{pv} \right) \right] \end{aligned}$$

where $\partial_\alpha \theta$ is denoted in appendix A.1

Appendix C

Matrices in FE-formulation

If plain strain is considered, a matrix format of the second-Piola Kirchhoff stress tensor and Green-Lagrange's tensor is introduced to suit computer implementation

$$\mathbf{S} = \begin{bmatrix} S_{xx} \\ S_{yy} \\ S_{xy} \end{bmatrix} \quad \delta \mathbf{E} = \begin{bmatrix} \delta E_{xx} \\ \delta E_{yy} \\ \delta E_{xy} \end{bmatrix}.$$

If all the elements in the Green-Lagrange's strain in terms of displacements is expanded the result is

$$\delta \mathbf{E} = \begin{bmatrix} \frac{\partial \delta u_x}{\partial x^o} \\ \frac{\partial \delta u_y}{\partial y^o} \\ \frac{\partial \delta u_x}{\partial y^o} + \frac{\partial \delta u_y}{\partial x^o} \end{bmatrix} + \begin{bmatrix} \frac{\partial u_x}{\partial x^o} \frac{\partial \delta u_x}{\partial x^o} + \frac{\partial u_y}{\partial x^o} \frac{\partial \delta u_y}{\partial x^o} \\ \frac{\partial u_x}{\partial y^o} \frac{\partial \delta u_x}{\partial y^o} + \frac{\partial u_y}{\partial y^o} \frac{\partial \delta u_y}{\partial y^o} \\ \frac{\partial \delta u_x}{\partial x^o} \frac{\partial u_x}{\partial y^o} + \frac{\partial u_x}{\partial x^o} \frac{\partial \delta u_x}{\partial y^o} + \frac{\partial \delta u_y}{\partial x^o} \frac{\partial u_y}{\partial y^o} + \frac{\partial \delta u_y}{\partial x^o} \frac{\partial u_y}{\partial x^o} \end{bmatrix} \quad (\text{C.1})$$

Introducing

$$\tilde{\nabla}_o = \begin{bmatrix} \frac{\partial}{\partial x^o} & 0 \\ 0 & \frac{\partial}{\partial y^o} \\ \frac{\partial}{\partial y^o} & \frac{\partial}{\partial x^o} \end{bmatrix} \quad \bar{\nabla}_o = \begin{bmatrix} \frac{\partial}{\partial x^o} & 0 \\ \frac{\partial}{\partial y^o} & 0 \\ 0 & \frac{\partial}{\partial x^o} \\ 0 & \frac{\partial}{\partial y^o} \end{bmatrix} \quad (\text{C.2})$$

and

$$\mathbf{A}(\mathbf{u}) = \begin{bmatrix} \frac{\partial u_x}{\partial x^o} & 0 & \frac{\partial u_y}{\partial x^o} & 0 \\ 0 & \frac{\partial u_x}{\partial y^o} & 0 & \frac{\partial u_y}{\partial y^o} \\ \frac{\partial u_x}{\partial y^o} & \frac{\partial u_x}{\partial x^o} & \frac{\partial u_y}{\partial y^o} & \frac{\partial u_y}{\partial x^o} \end{bmatrix} \quad (\text{C.3})$$

this yields that the variation of the Green-Lagrange's strain can be written in a compact way

$$\delta \mathbf{E} = \tilde{\nabla}_0 \delta \mathbf{u} + \mathbf{A}(\mathbf{u}) \bar{\nabla} \delta \mathbf{u} \quad (\text{C.4})$$

The surface traction, the body force, the displacement and the arbitrary displacement in matrix form are

$$\mathbf{u} = \begin{bmatrix} u_x \\ u_y \end{bmatrix} \quad \mathbf{t}^0 = \begin{bmatrix} t_x^0 \\ t_y^0 \end{bmatrix} \quad \mathbf{b} = \begin{bmatrix} b_x^0 \\ b_y^0 \end{bmatrix} \quad \delta \mathbf{u} = \begin{bmatrix} \delta u_x \\ \delta u_y \end{bmatrix}$$

Discrete approximation of the displacement field and variation of displacement field can be achieved by using form functions for, for example four node elements as

$$\mathbf{u} = \begin{bmatrix} \mathbf{N}_1(\mathbf{x}^0) \\ \mathbf{N}_2(\mathbf{x}^0) \end{bmatrix} \hat{\mathbf{u}} = \mathbf{N}(\mathbf{x}^0) \hat{\mathbf{u}} \quad \delta \mathbf{u} = \mathbf{N}(\mathbf{x}^0) \delta \hat{\mathbf{u}}$$

where \mathbf{N} are the form functions.

Inserting this into the variation of the Green-Lagrange's strain (C.4) yields

$$\delta \mathbf{E} = (\mathbf{B}_0^l + \mathbf{A}(\mathbf{u}) \mathbf{H}_0) \delta \hat{\mathbf{u}} = \mathbf{B}_0 \delta \hat{\mathbf{u}} \quad (\text{C.5})$$

where

$$\mathbf{B}_0^l = \tilde{\nabla}_0 \mathbf{N} \quad \text{and} \quad \mathbf{H}_0 = \bar{\nabla}_0 \mathbf{N}.$$

Inserting the form functions for e.g. a 4-node element on element level, these matrices are explicitly written as

$$\mathbf{B}_o^{le} = \begin{bmatrix} \frac{\partial N_1}{\partial x^o} & 0 & \frac{\partial N_2}{\partial x^o} & 0 & \frac{\partial N_3}{\partial x^o} & 0 & \frac{\partial N_4}{\partial x^o} & 0 \\ 0 & \frac{\partial N_1}{\partial y^o} & 0 & \frac{\partial N_2}{\partial y^o} & 0 & \frac{\partial N_3}{\partial y^o} & 0 & \frac{\partial N_4}{\partial y^o} \\ \frac{\partial N_1}{\partial y^o} & \frac{\partial N_1}{\partial x^o} & \frac{\partial N_2}{\partial y^o} & \frac{\partial N_2}{\partial x^o} & \frac{\partial N_3}{\partial y^o} & \frac{\partial N_3}{\partial x^o} & \frac{\partial N_4}{\partial y^o} & \frac{\partial N_4}{\partial x^o} \end{bmatrix} \quad (\text{C.6})$$

$$\mathbf{H}_o^e = \begin{bmatrix} \frac{\partial N_1}{\partial x^o} & 0 & \frac{\partial N_2}{\partial x^o} & 0 & \frac{\partial N_3}{\partial x^o} & 0 & \frac{\partial N_4}{\partial x^o} & 0 \\ \frac{\partial N_1}{\partial y^o} & 0 & \frac{\partial N_2}{\partial y^o} & 0 & \frac{\partial N_3}{\partial y^o} & 0 & \frac{\partial N_4}{\partial y^o} & 0 \\ 0 & \frac{\partial N_1}{\partial x^o} & 0 & \frac{\partial N_2}{\partial x^o} & 0 & \frac{\partial N_3}{\partial x^o} & 0 & \frac{\partial N_4}{\partial x^o} \\ 0 & \frac{\partial N_1}{\partial y^o} & 0 & \frac{\partial N_2}{\partial y^o} & 0 & \frac{\partial N_3}{\partial y^o} & 0 & \frac{\partial N_4}{\partial y^o} \end{bmatrix}. \quad (\text{C.7})$$